EXAMINATION OF CURING CRITERIA FOR COLD IN-PLACE RECYCLING
Phase 2: Measuring Temperature, Moisture, Deflection and Distress from CIR Test Section

Final Report
March 2009

Conducted by
Hosin "David" Lee
Yongjoo "Thomas" Kim
Soohyok "Dan" Im

Public Policy Center
University of Iowa

Disclaimer Notice

The contents of this report reflect the views of the authors, who are responsible for the facts and the accuracy of the information presented herein. The opinions, findings, and conclusions expressed in this publication are those of the authors and not necessarily those of the sponsors.   The sponsors assume no liability for the contents or use of the information contained in this document. This report does not constitute a standard, specification, or regulation. The sponsors do not endorse products or manufacturers. Trademarks or manufacturers' names appear in this report only because they are considered essential to the objectives of the document.

Non-discrimination Statement

Federal and state laws prohibit employment and/or public accommodation discrimination on the basis of age, color, creed, disability, gender identity, national origin, pregnancy, race, religion, sex, sexual orientation or veteran's status. If you believe you have been discriminated against, please contact the Iowa Civil Rights Commission at 800-457-4416 or Iowa Department of Transportation's affirmative action officer. If you need accommodations because of a disability to access the Iowa Department of Transportation's services, contact the agency's affirmative action officer at 800-262-0003.

1. REPORT NO. IHRB Report TR-590	2. GOVERNMENT ACCESSION NO.	3. RECIPIENT'S CATALOG NO.
4. TITLE AND SUBTITLE Examination of Curing Criteria for Cold In-Place Recycling (Phase 2: Measuring Temperature, Moisture, Deflection and Distress from CIR Test Section)		5. REPORT DATE March 2009
		6. PERFORMING ORGANIZATION CODE
7. AUTHOR(S) Hosin "David" Lee, Yongjoo "Thomas" Kim, and Soohyok "Dan" Im		8. PERFORMING ORGANIZATION REPORT NO.
9. PERFORMING ORGANIZATION NAME AND ADDRESS Public Policy Center University of Iowa 227 South Quadrangle Iowa City, IA 52242-1192		10. WORK UNIT NO.
		11. CONTRACT OR GRANT NO
12. SPONSORING AGENCY NAME AND ADDRESS Iowa Highway Research Board Iowa Department of Transportation 800 Lincoln Way, Ames, IA 50010		13. TYPE OF REPORT AND PERIOD COVERED Final Report
		14. SPONSORING AGENCY CODE

15. SUPPLEMENTARY NOTES

16. ABSTRACT

The previous research performed laboratory experiments to measure the impacts of the curing on the indirect tensile strength of both CIR-foam and CIR-emulsion mixtures. However, a fundamental question was raised during the previous research regarding a relationship between the field moisture content and the laboratory moisture content. Therefore, during this research, both temperature and moisture conditions were measured in the field by embedding the sensors at a midpoint and a bottom of the CIR layer. The main objectives of the research are to: (1) measure the moisture levels throughout a CIR layer and (2) develop a moisture loss index to determine the optimum curing time of CIR layer before HMA overlay.

To develop a set of moisture loss indices, the moisture contents and temperatures of CIR-foam and CIR-emulsion layers were monitored for five months. Based on the limited field experiment, the following conclusions are derived:

1. The moisture content of the CIR layer can be monitored accurately using the capacitance type moisture sensor.
2. The moisture loss index for CIR layers is a viable tool in determining the optimum timing for an overlay without measuring actual moisture contents.
3. The modulus back-calculated based on the deflection measured by FWD seemed to be in a good agreement with the stiffness measured by geo-gauge.
4. The geo-gauge should be considered for measuring the stiffness of CIR layer that can be used to determine the timing of an overlay.
5. The stiffness of CIR-foam layer increased as a curing time increased and it seemed to be more influenced by a temperature than moisture content.

The developed sets of moisture loss indices based on the field measurements will help pavement engineers determine an optimum timing of an overlay without continually measuring moisture conditions in the field using a nuclear gauge.

17. KEY WORDS cold in-place recycling, curing criteria, moisture content, curing time, moisture loss index, geo-gauge		18. DISTRIBUTION STATEMENT No restrictions.	
19. SECURITY CLASSIF. (of this report) None	20. SECURITY CLASSIF. (of this page) None	21. NO. OF PAGES 59	22. PRICE N/A

Examination of Curing Criteria for Cold In-Place Recycling
(Phase 2: Measuring Temperature, Moisture, Deflection and Distress from CIR Test Section)

Final Report
March 2009

Principal Investigator

Hosin "David" Lee, Ph. D., P. E.

Associate Professor

Public Policy Center, Department of Civil and Environmental Engineering,

University of Iowa

Researcher

Yongjoo "Thomas" Kim, Ph. D.

Postdoctoral Research Scholar

Public Policy Center, Department of Civil and Environmental Engineering,

University of Iowa

Research Assistants

Soohyok "Dan" Im

Graduate Research Assistant

Public Policy Center, Department of Civil and Environmental Engineering,

University of Iowa

Technical Advisory Committee

Bob Nady, Consultant, rmnady@midiowa.net

Bill Kahl, W.K. Construction, wkc@chorus.net

Bill Rosener, APAI, billr@apai.net

Greg Parker, Johnson County, gparker@co.johnson.ia.us

John Hinrichsen, Iowa DOT, John.Hinrichsen@dot.iowa.gov

Larry Mattusch, APAI, lmatt2@mchsi.com

Mark Haines, Koss Construction, mah@kossconstruction.com

Mike Heitzman, NCAT, mah0016@auburn.edu

Scott Schram, Iowa DOT, Scott.Schram@dot.iowa.gov

Steve Buckner, Flint Hills Resources, Steve.Buckner@fhr.com

Table of Contents

LIST OF TABLES

LIST OF FIGURES

1. INTRODUCTION

The previous research performed laboratory experiments to measure the impacts of the curing on the indirect tensile strength of both CIR-foam and CIR-emulsion mixtures. However, a fundamental question was raised regarding a relationship between field moisture content and the laboratory moisture content in gyratory compacted specimens cured under varying temperature and moisture conditions.   To develop moisture loss index, both moisture content and temperature were measured from the CIR projects in the field.

1.1 Objectives

The main objectives of the research are to: (1) measure the moisture levels throughout a CIR layer and (2) develop a moisture loss index to determine the optimum curing time of CIR layer before HMA overlay.

1.2 Benefits of the Study

During the previous research, efforts were made on the laboratory experimentation. During this research, both moisture and temperature conditions were measured in the field by embedding the moisture meter and temperature sensor at a midpoint and a bottom of the CIR layer.   The results of the research are presented as a set of moisture loss indices based on the field measurements that will help pavement engineers determine an optimum timing of an HMA overlay without continually measuring moisture conditions in the field using a nuclear gauge.

2. SUMMARY FROM THE PREVIOUS STUDY

The previous research effort focused on laboratory curing procedures to simulate the moisture loss of the CIR layer in the field.   To represent the curing process of CIR layer in the field construction, three different laboratory curing procedures were examined: (1) uncovered, (2) semi-covered and (3) covered specimens.   Indirect tensile strengths and moisture contents of the CIR specimens cured for various curing periods were measured. To predict the field performance of CIR pavements during the curing process, dynamic modulus and dynamic creep tests were conducted using Superpave simple performance testing (SPT) equipment.

The indirect tensile strength of CIR specimens in all three curing conditions did not increase during the early stage of curing but increased during a later stage of curing, usually when the moisture content fell below 1.5%.   Dynamic modulus and flow number increased as curing time increased and moisture content decreased.   For the same curing time, CIR-foam specimens exhibited the higher tensile strength, dynamic modulus and flow number than CIR-emulsion.   This might have been caused by the higher moisture content in the CIR-emulsion specimens than the CIR-foam for the equivalent curing time.   The laboratory test results concluded that method, temperature, and length of curing significantly affected the properties of the CIR mixtures.   In order to develop a better analysis tool to monitor the CIR layer in preparation for timely placement of the wearing surface, the concept of a moisture loss index was explored.

3. MOISTURE METERS

Two CIR-emulsion and CIR-foam project sites were identified for monitoring moisture content and temperature in the field.   Two types of dielectric moisture sensors were used to measure the moisture content from CIR layer in the field: (1) Portable time domain reflectometer (TDR) device and (2) Capacitance moisture sensor.   A TDR sensor measures the dielectric constant of a CIR layer by measuring a time for an electromagnetic pulse to traverse in the CIR layer.   The capacitance moisture sensor is based on the capacitance that measures the dielectric constant of a CIR layer by finding the rate of change of voltage on a sensor.

3.1 Time Domain Reflectometer (TDR)

Time domain reflectometry (TDR) probes have been widely used to detect the in-situ moisture content in soils since the late 1970s.   The TDR uses the propagation of electromagnetic wave that is affected by a presence of water.   Jiang et al. (1999) reported that TDR was a reliable means to determine in-situ soil moisture content.   Yu et al. (2008) developed a method to directly estimate the degree of freeze/thaw from a TDR measurement.   Hanek et al. (2001) reported that monitoring soil moisture using TDR could provide a method for determining the timing when the heavy loads could be applied.   Liang et al. (2006) found that the variations in the moisture content at the base and subbase layers could give an indication on how fast the surface material can drain water.   Lee et al. (2008) applied a micromechanics scheme to consider variations of dry density in computing a volume of water.

For this research, a portable TDR device was used to measure moisture content of CIR layer in the field.   Figure 3-1 shows the potable TDR 300 device along with its specification for measuring the moisture content through two rods penetrated from the surface of a CIR layer.

Specification	
Measurement Units	Percent volumetric water content
Resolution	0.1%
Accuracy	±3.0% volumetric water content with electrical conductivity < 2 dS m −1
Range	0% to saturation (Saturation is typically around 50% volumetric water)
Power	4 AAA alkaline batteries (Approximately 12 month life)
Logger Capacity	2700 readings without GPS, 1250 readings with GPS/DGPS
Display	16 character, 2 line LCD
Weight	3 lbs.
Probe Head Dimensions	3.1" x 3" x 1"
Rod Dimensions	- Length : 3", 4.7" or 7.9" - Diameter: 0.2" - Spacing: 1.3"

Figure 3-1. Portable TDR moisture meter and specification

3.2 Capacitance Moisture Sensor

As shown in Figure 3-2, a capacitance moisture sensor consists of a pair of electrodes (either an array of parallel spikes or circular metal rings) which form a capacitor with the soil acting as the dielectric in between.   This capacitor works with the oscillator to form a tuned circuit and measures changes in soil water content by detecting changes in the operating frequency.   Advantages and disadvantages of a capacitance moisture sensor are summarized below.

4
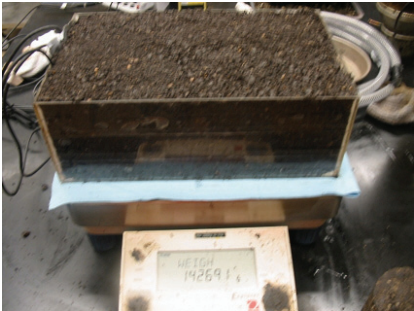
	Specifications
Measurement Time	10ms (milliseconds)
Accuracy	at least 0.003 m^3/m^3 all soils, up to 8 dS/m With soil-specific calibration: $\pm.02$ m^3/m^3 ($\pm2\%$)
Resolution	0.001 m^3/m^3 VWC in mineral soils, 0.25% in growing media
Power	3VDC @ 10mA *Output:* 10-40% of excitation voltage (250-1000mV at 2500mV excitation)
Operating Environment	-40°C to +60 °C

Figure 3-2. Capacitance sensors and specification

Generally capacitance moisture sensors operate at lower frequencies (100MHz or less) and can therefore detect "bound" water in fine-particle soils. This bound water is water that is strongly attracted to the surface of soil particles and can constitute more than 10% soil moisture content. Much of this bound water is available to plants, but is not detected effectively by TDR systems operating at frequencies > 250MHz. Systems operating at lower frequencies (particularly at < 20MHz) are more susceptible to soil salinity errors. Readings are heavily influenced by moisture content and air gaps in the soil volume near the electrodes (this is also true with TDR systems).

4. LABORATORY EVALUATION OF CAPACITANCE MOISTURE SENSOR

As shown in Figure 4-1, a laboratory CIR-emulsion specimen was prepared in the rectangular plastic container.   CSS-1h emulsion with an asphalt content of 3.0% and additional water at 10% of RAP weight were added.   Three capacitance moisture sensors were buried at 2.0, 3.0 and 4.5 inches from the surface and the specimen was then compacted using a manual Marshall hammer.   As summarized in Figure 4-1, moisture contents of 2.8% and 4.9% and 7.3% were measured from the sensors buried at 2.0, 3.0 and 4.5 inches, respectively.   An average value of these three moisture contents matched reasonably well with the actual moisture content of 4.2% for the specimen.

	Sensor location from surface	Measured moisture content from sensor after 10 days	Measured moisture content from real weight
	2.0 in.	2.8%	
	3.0 in.	4.9%	4.2%
	4.5 in.	7.3%	

Figure 4-1. Three sensors buried in CIR-emulsion specimen in the laboratory

5. MEASUREMENT OF MOISTURE CONTENT USING TIME DOMAIN REFLECTOMETER (TDR) FROM COLD IN-PLACE RECYCLING WITH FOAMED ASPHALT

First, a pilot study was conducted to examine the testing device and monitoring plan from the CIR-foam project site in Cedar County.   Figure 5-1 depicts activities performed during the pilot study.
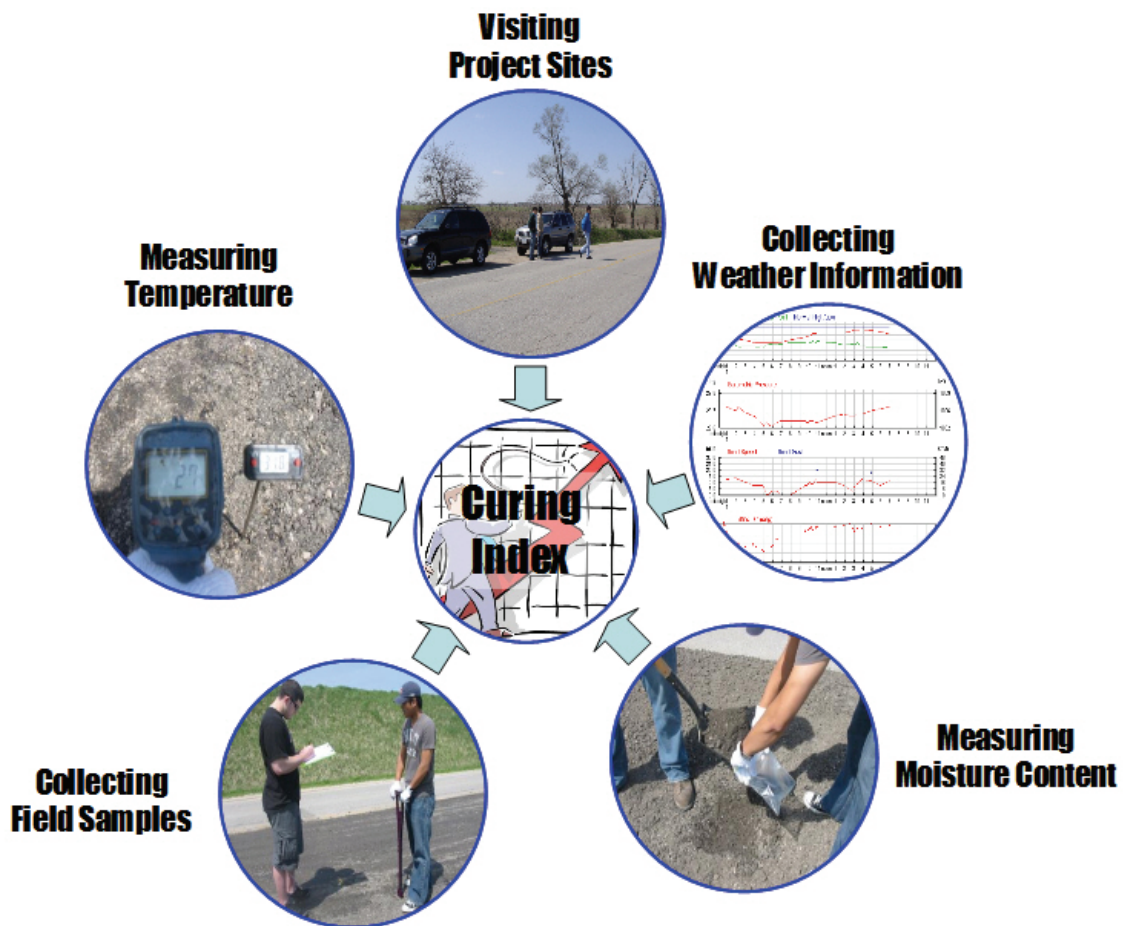
Figure 5-1. Diagram of work plan for pilot study

5.1 Description of CIR-foam Project in Cedar County

As shown in Figure 5-2, CIR-foam project site is located from south of the city of West Branch to the Cedar-Muscatine County line, Iowa.   As shown in Figure 5-3, 4.3-mile section of County Road X 30 was rehabilitated from I-80 to SH-6 using the CIR-foam process between May 5th and May 9th, 2008.   As shown in Figure 5-4 (a), the top four inches of the existing 9-inch thick Type B HMA layer were milled and mixed with foamed asphalt to produce 4-inch thick CIR-foam layer.   Upon completion of tack coating process on top of CIR-foam layer (Figure 5-4 (b)), 1.5-inch thick HMA intermediate course was overlaid on May 15th, 2008 (Figure 5-4 (c)) followed by 1.5-inch thick HMA wearing course overlaid on May 22nd, 2008 (Figure 5-4 (d)).

Figure 5-2. Locations of CIR-foam project sites for pilot study

Figure 5-3. Comparison of pavement cross section of CIR-foam project site in Cedar County

(a) CIR-foam process

(b) Tack coating process

(c) Intermediate HMA overlay process

(d) Wearing HMA overlay process

Figure 5-4. Pictures of CIR-foam, tack coating, and HMA overlay processes

5.2 Survey of Existing Pavement Condition

As shown in Figure 5-5, the research team visited the County Road X 30 before performing a CIR-foam construction in Cedar County.   As shown in Figure 5-6, a relatively small amount of transverse cracks were observed at a uniform interval and a limited amount of longitudinal cracks were also observed.

Figure 5-5. Pictures of visiting project sites before construction

Figure 5-6. Pictures of surface conditions of the existing pavement

11

5.3 Collection of CIR-foam Mixture

To measure the moisture content of CIR-foam field mixtures in the laboratory, as shown in Figure 5-7, CIR-foam mixtures were collected from six different locations between 10:00 a.m. to 12:00 p.m. and between 4:00 p.m. to 6:00 p.m. on May 6th-8th, 2008. Table 5-1 summarizes the laboratory moisture contents of CIR-foam field mixtures that were collected from six locations.   The average moisture content of 2.2% measured at University of Iowa is in a good agreement with 2.4% as measured by a contractor.
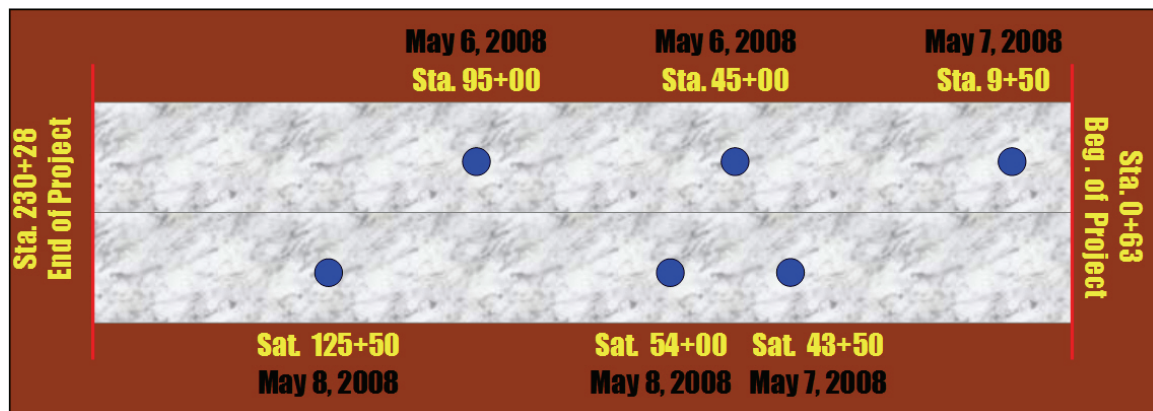
Figure 5-7. Locations where CIR-foam field mixtures were collected

Table 5-1. Laboratory moisture content of CIR-foam field mixtures

Station No.	University of Iowa				Contractor
	# 1	# 2	# 3	Average	Average
95+00	2.0%	1.7%	2.0%	1.9%	2.2%
45+00	1.7%	3.8%	2.0%	2.5%	2.2%
9+50	2.5%	2.3%	1.7%	2.2%	2.7%
43+50	2.3%	2.1%	1.8%	2.1%	2.6%
54+00	2.0%	1.5%	2.2%	1.9%	2.6%
125+00	2.7%	2.4%	2.1%	2.4%	2.6%
			Total Average	2.2%	2.4%

5.4 Measurement of Field Moisture Content and Temperature

As shown in Figure 5-8, both moisture contents and temperatures were measured from seven different locations between 10:00 a.m. to 12:00 p.m. and between 4:00 p.m. to 6:00 p.m. for eleven days between May 5th and 15th, 2008.   As shown in Figure 5-9, nine measurements were made from each location and their average value was recorded for each day in Table 5-2.   Figure 5-10 shows a plot of moisture contents measured between May 5th and May 15th 2008.   Figure 5-11 shows plots of field moisture contents measured by a potable TDR device against field moisture content measured by a nuclear gauge.   It should be noted that the moisture contents measured using a portable TDR device and a nuclear gauge represent the average moisture condition between the surface and 1.5 inch to 2.0 inch from the surface and they were all above the minimum moisture content of 1.5% that is required for an HMA overlay.

As shown in Figure 5-12, temperatures were measured nine times for each location and the average value was recorded for each day in Table 5-3.   Figure 5-13 shows a plot of temperatures from May 5th to May 15th 2008.
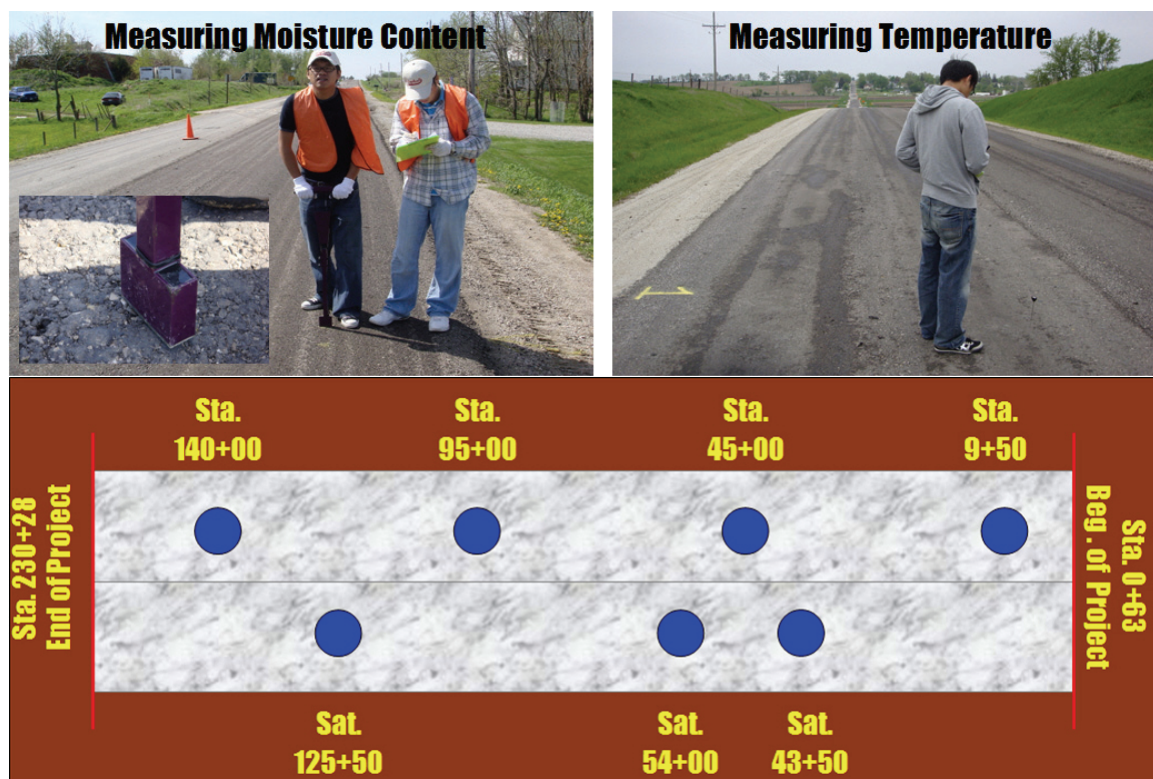
Figure 5-8. Locations where moisture contents and temperatures were measured
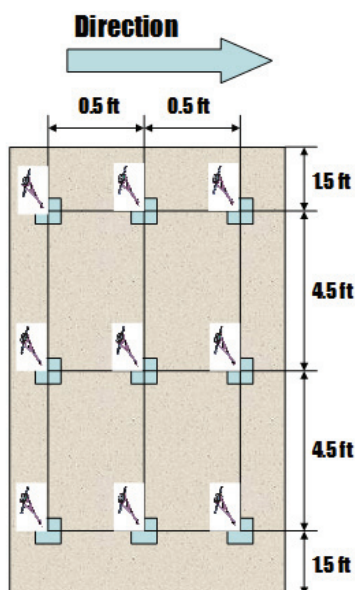
Figure 5-9. Nine moisture measurements for each location using a portable TDR

Table 5-2. Field moisture contents of CIR-foam layer

Date	Station No.						
	140+00	95+00	45+00	9+50	43+50	54+00	125+00
May 5 (Sunny)	2.6%	-	-	-	-	-	-
May 6 (Sunny)	2.6%	-	-	-	-	-	-
May 7 (Sunny)	2.8%	3.5%	3.2%	2.2%	2.6%	-	-
May 8 (Sunny)	-	-	-	-	2.3%	2.5%	2.8%
May 9 (Sunny)	-	3.0%	3.3%	1.7%	2.0%	2.6%	2.7%
May 10 (Rain)	2.8%	3.9%	3.3%	2.4%	2.7%	2.9%	2.7%
May 11 (Rain)	4.2%	4.7%	4.9%	3.3%	4.8%	5.0%	5.8%
May 12 (Sunny)	3.6%	4.0%	4.1%	3.1%	3.6%	3.9%	4.1%
May 13 (Rain)	4.1%	4.6%	4.6%	3.0%	4.0%	4.3%	4.4%
May 14 (Sunny)	3.2%	4.2%	3.3%	2.5%	3.2%	3.6%	3.6%
May 15 (Sunny)	2.7%	3.2%	3.2%	1.9%	2.9%	3.0%	3.4%
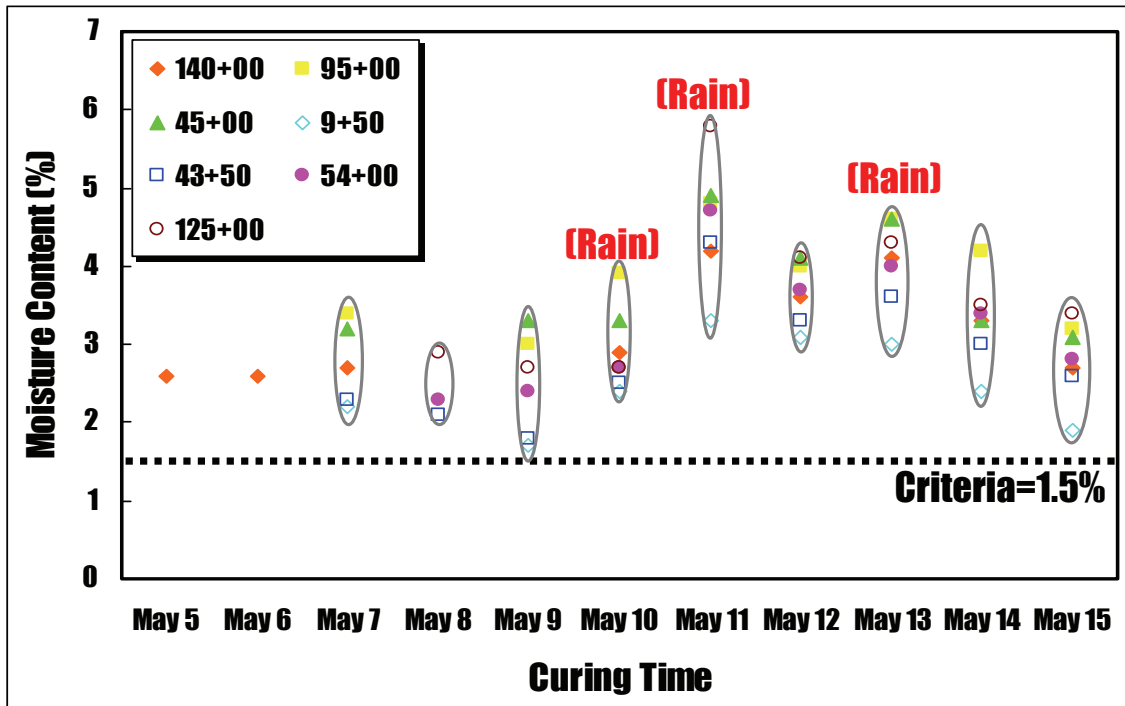
Figure 5-10. Plots of field moisture contents measured by a portable TDR

Station No.	Date Measured	TDR Device	Nuclear Gauge
140+00	May 6	2.6%	1.4%
95+00	May 7	3.5%	4.7%
45+00	May 7	3.2%	4.8%
9+50	May 9	1.7%	2.6%
43+50	May 9	2.0%	3.1%
54+00	May 9	2.6%	2.0%
125+00	May 9	2.7%	2.0%
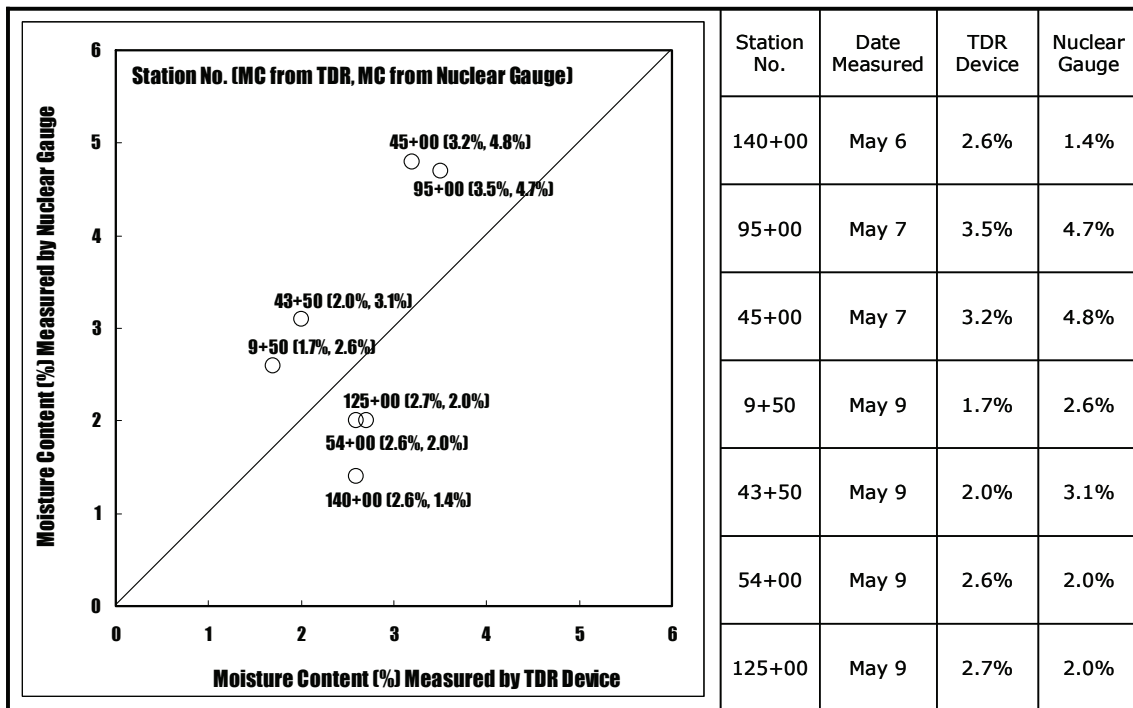
Figure 5-11. Plots of field moisture content measured by a portable TDR against field moisture content measured by a nuclear gauge
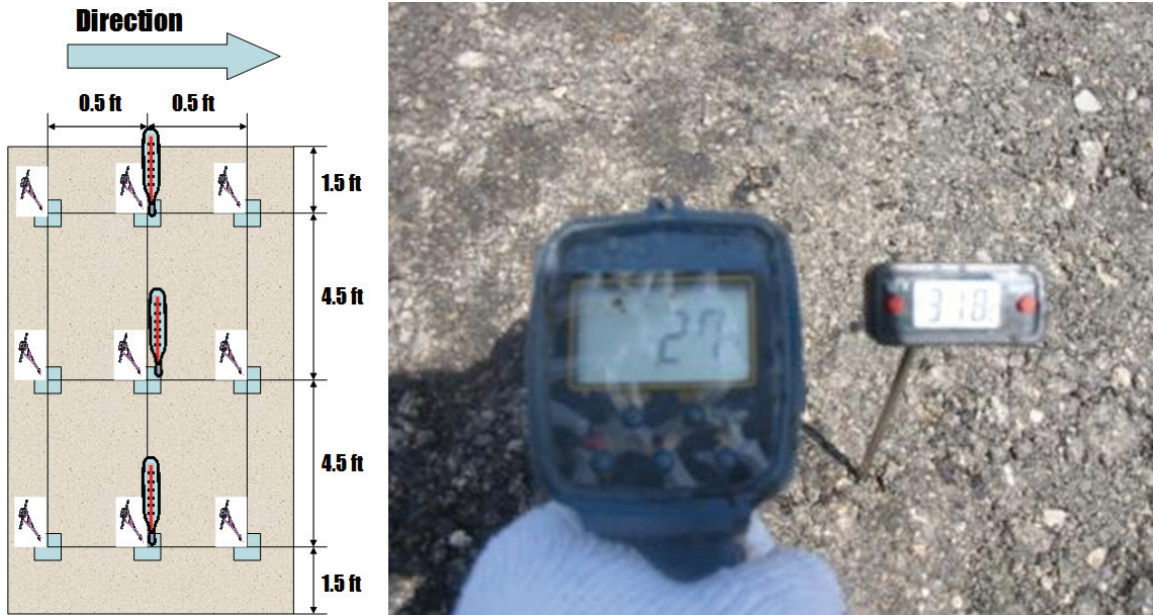
Figure 5-12. Nine measurements for measuring CIR-foam layer temperature

Table 5-3. Field temperatures of CIR-foam layer

Date	Station No.						
	140+00	95+00	45+00	9+50	43+50	54+00	125+00
May 5 (Sunny)	80.1°F	-	-	-	-	-	-
May 6 (Sunny)	92.3°F	-	-	-	-	-	-
May 7 (Sunny)	79.2°F	76.5°F	77.0°F	80.1°F	89.8°F	-	-
May 8 (Sunny)	-	-	-	-	89.4°F	88.3F	81.5°F
May 9 (Sunny)	-	82.8°F	79.0°F	82.2°F	83.8°F	85.1°F	82.0°F
May 10 (Rain)	80.2°F	79.3°F	70.1°F	70.1°F	82.9°F	77.5°F	75.0°F
May 11 (Rain)	66.9°F	64.8°F	62.6°F	65.3°F	65.1°F	64.2°F	62.8°F
May 12 (Sunny)	85.5°F	84.9°F	81.9°F	88.3°F	88.3°F	85.5°F	77.0°F
May 13 (Rain)	67.3°F	67.5°F	65.8°F	69.6°F	68.7°F	68.7°F	65.5°F
May 14 (Sunny)	88.2°F	87.6°F	84.2°F	87.4°F	85.6°F	87.8°F	83.1°F
May 15 (Sunny)	79.9°F	79.5°F	73.4°F	75.2°F	76.5°F	75.4°F	73.2°F
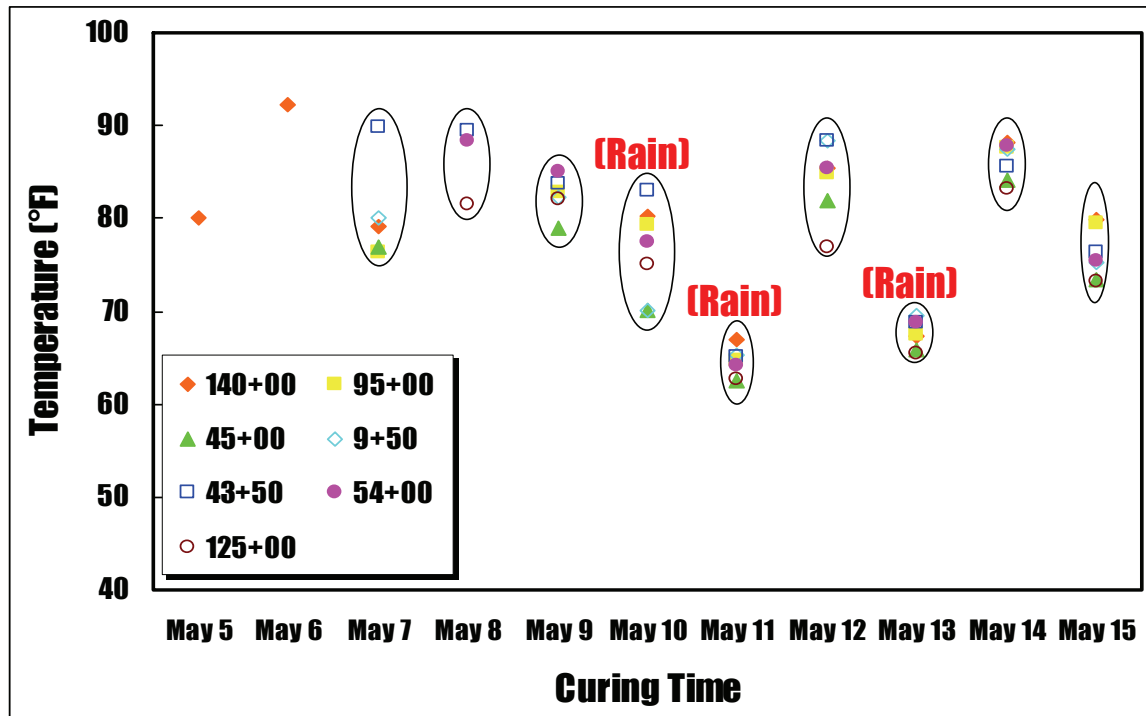
Figure 5-13. Plots of field temperature measured from CIR-foam layer

5.5 Observation of CIR-foam Layer Stiffness

Table 5-4 illustrates different approaches to measuring the moisture contents in CIR-foam layer.   During cool days, two rods of a portable TDR could not penetrate the CIR-foam layer and the CIR-foam layer was drilled to create holes for the TDR probes.   As can be seen in Table 5-4, the stiffness of CIR-foam layer was not affected by the moisture content in the CIR-foam layer but CIR-foam layer was affected by its temperature.   The stiffness of the CIR layer may not be a good measure of moisture loss but may be used as a measure to determine the optimum timing of an overlay.

17

Table 5-4. Observation of CIR-foam layer stiffness

Moisture Measuring Process	Date	Range of moisture content	Range of CIR-foam layer temperature
Drill + TDR	May 10	2.7%–3.9%	70.1°F–80.2°F
	May 11	3.3%–5.8%	62.6°F–66.9°F
	May 13	3.0%–4.6%	65.5°F–69.6°F
	May 15	1.9%–3.4%	73.2°F–79.9° F
TDR	May 9	1.7%–3.3%	79.0°F–85.1°F
	May 12	3.1%–4.1%	77.0°F–88.3°F
	May 14	2.5%–4.2%	83.1°F–87.6°F

6. MEASUREMENT OF MOISTURE CONTENT USING MOISTURE SENSORS FROM COLD IN-PLACE RECYCLING WITH EMULSIFIED ASPHALT

To measure the field moisture contents and temperature of CIR-emulsion layer, as shown in Figure 6-1, cold in-place recycling with CSS-1 emulsified asphalt (CSS-1-emulsion) project site in Scott County was selected. CIR-CSS-1-emulsion project site is located from Iowa Highway 22 in the town of Buffalo to Mayne Street in the town of Blue Grass, Iowa.
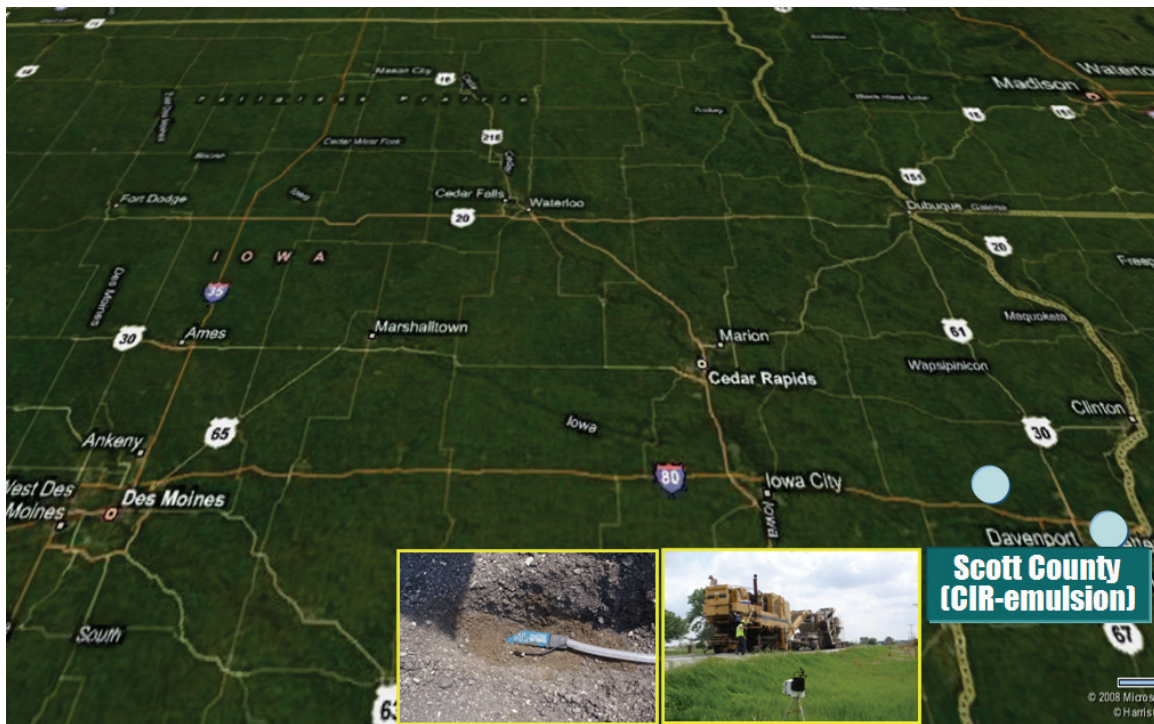
Figure 6-1. Locations of CIR-CSS-1-emulsion project sites in Scott County

6.1 Description of CIR-CSS-1-emulsion Project in Scott County

As shown in Figure 6-2, 2.5-mile section of County Road Y-40 was rehabilitated from Iowa Highway 22 in the town of Buffalo to Mayne Street in the town of Blue Grass, Iowa between June 5th and June 6th, 2008.

As shown in Figure 6-3 (a), all four inches of the existing Type B HMA layer on top of

19

the concrete pavement were milled and mixed with CSS-1 emulsified asphalt to produce 4-inch thick CIR-CSS-1-emulsion layer. 2.0-inch thick HMA intermediate course was overlaid on June 26th, 2008 (Figure 6-3 (c)) followed by 1.5-inch thick HMA wearing course overlaid on July 3rd, 2008 (Figure 6-3 (d)).

Figure 6-2. Comparison of pavement cross section of CIR-CSS-1-emulsion project site in Scott County

(a) CIR-emulsion process

(b) Tack coating process

(c) Intermediate HMA overlay process

(d) Wearing HMA overlay process

Figure 6-3. Pictures of CIR-CSS-1-emulsion, tack coating, and HMA overlay processes

6.2 Survey of Existing Pavement Condition

2.5-mile section of County Road Y-40 was surveyed before it was rehabilitated.   As shown in Figure 6-4, a large amount of transverse cracks were observed at a uniform interval and an extensive amount of longitudinal cracks were also observed.

(a) Longitudinal crack

(b) Transverse cracks

Figure 6-4. Pictures of surface conditions on existing pavement

6.3 Collection of CIR-CSS-1-emulsion Mixture

To measure the moisture content of CIR-CSS-1-emulsion field mixtures in the laboratory, as shown in Figure 6-5, CIR-CSS-1-emulsion mixtures were collected from three different locations between 5:00 p.m. to 5:30 p.m. on June 5th, 2008.   Table 6-1 summarizes the laboratory moisture contents of CIR-CSS-1-emulsion field mixtures, which were collected from three locations.   The average moisture content of 2.8% measured at University of Iowa was significantly lower than 3.8% as measured by a contractor.

Figure 6-5. Locations where CIR-CSS-1-emulsion field mixtures were collected

Table 6-1. Laboratory moisture content of CIR-CSS-1-emulsion field mixtures

| Station No. | University of Iowa | | | | Contractor |
	# 1	# 2	# 3	Average	Average
102+00	2.0%	2.6%	1.9%	2.2%	
110+00	3.0%	2.8%	3.2%	3.0%	3.8%
129+00	4.3%	2.9%	2.4%	3.2%	
			Total Average	2.8%	3.8%

6.4 Measurement of Field Moisture Content and Temperature

To monitor actual moisture contents of the CIR-CSS-1-emulsion layer in the field, as shown in Figure 6-6 and Figure 6-7, three ECH_2O moisture sensors and two temperature sensors were installed at the bottom of CIR-CSS-1-emulsion layer.   A weather station was also installed to collect air temperature, humidity, rainfall and wind speed.

Figure 6-8, Figure 6-9, Figure 6-10, Figure 6-11, Figure 6-12 show plots of moisture content, temperature, rainfall, humidity, and wind speed, respectively, measured during the curing time of 19 days when fourteen rainfalls with a total amount of 6.38 inch had occurred.   The moisture contents at the bottom of CIR-CSS-1-emulsion layer before the intermediate HMA overlay were measure as 9.4% from sensor A, 11.1% from sensor B, and 9.4% from sensor C.   Despite the actual moisture content of CIR-CSS-1-emulsion layer being above 1.5%, the intermediate HMA overlay was constructed after 19 days of curing.   Figure 6-13 shows plots of temperature from three sensors embedded in the CIR-CSS-1-emulsion layer against air temperature from weather station device.   As shown in Figure 6-14, as expected, temperature of CIR-CSS-1-emulsion layer is higher than air temperature.
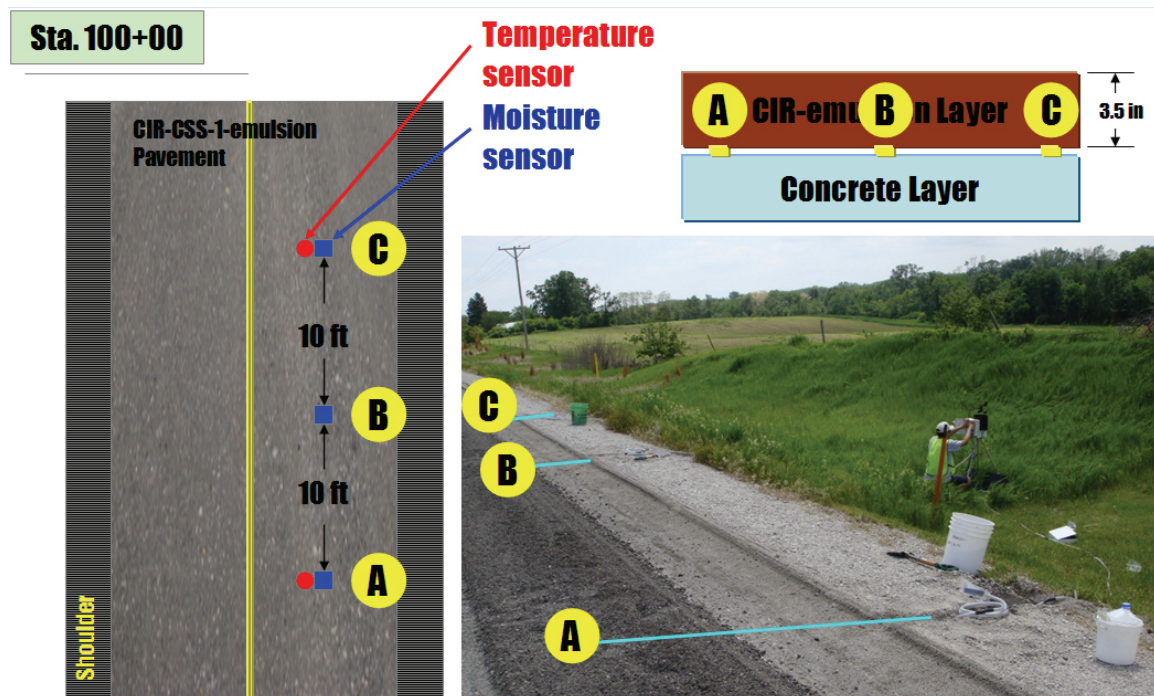
Figure 6-6. Embedded moisture and temperature sensors installed at the bottom of CIR-CSS-1-emulsion layer

24

(a) Selection of testing section
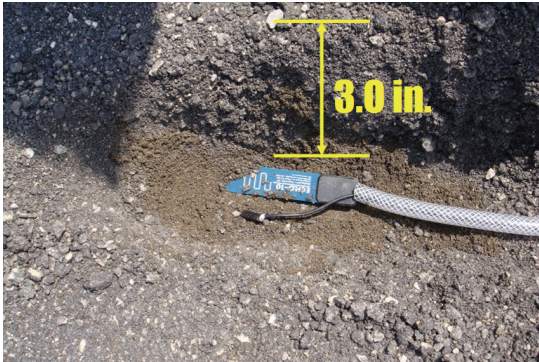
(b) Moisture and temperature sensors

(c) Installation of weather station

(d) Monitoring

Figure 6-7. Pictures of installation process for embedded moisture and temperature sensors at the bottom of the CIR-CSS-1-emulsion layer
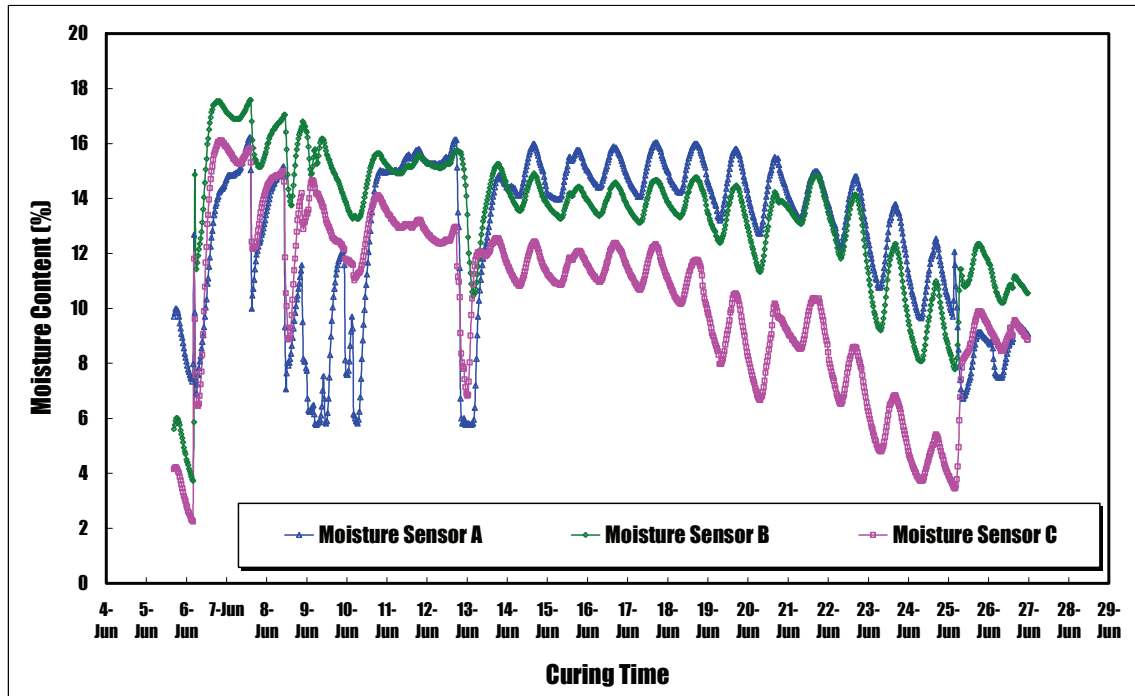
Figure 6-8. Plots of moisture contents against the curing time from three sensors embedded in the CIR-CSS-1-emulsion layer
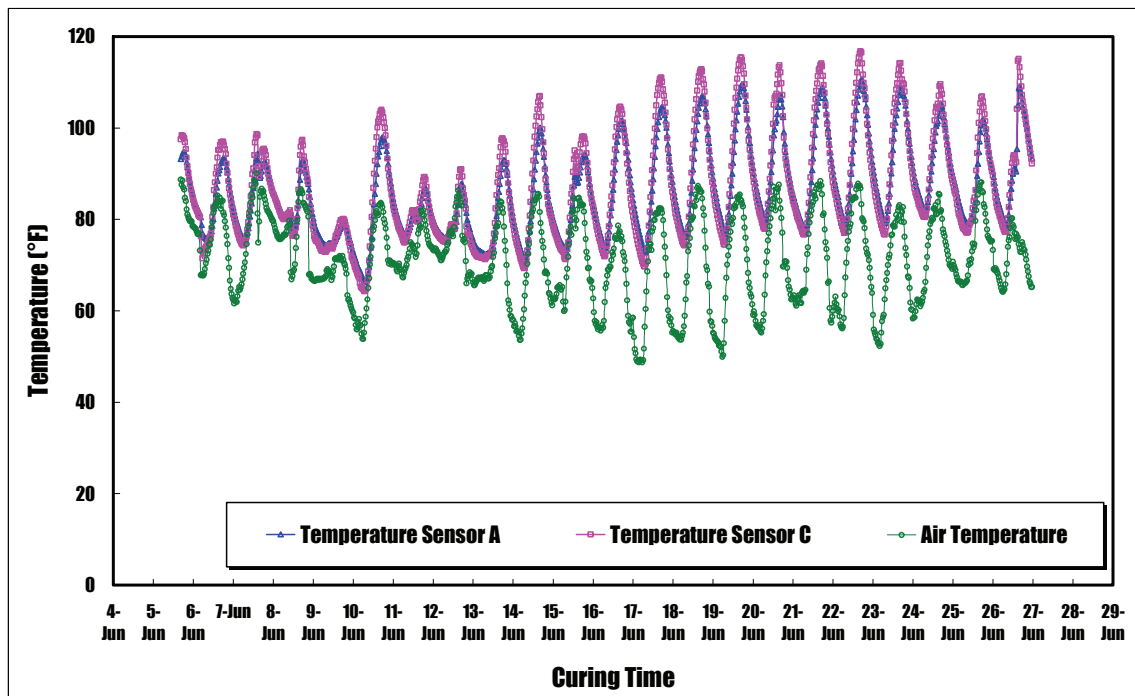
Figure 6-9. Plots of temperature against the curing time from two sensors embedded in the CIR-CSS-1-emulsion layer and air temperature from weather station device

26
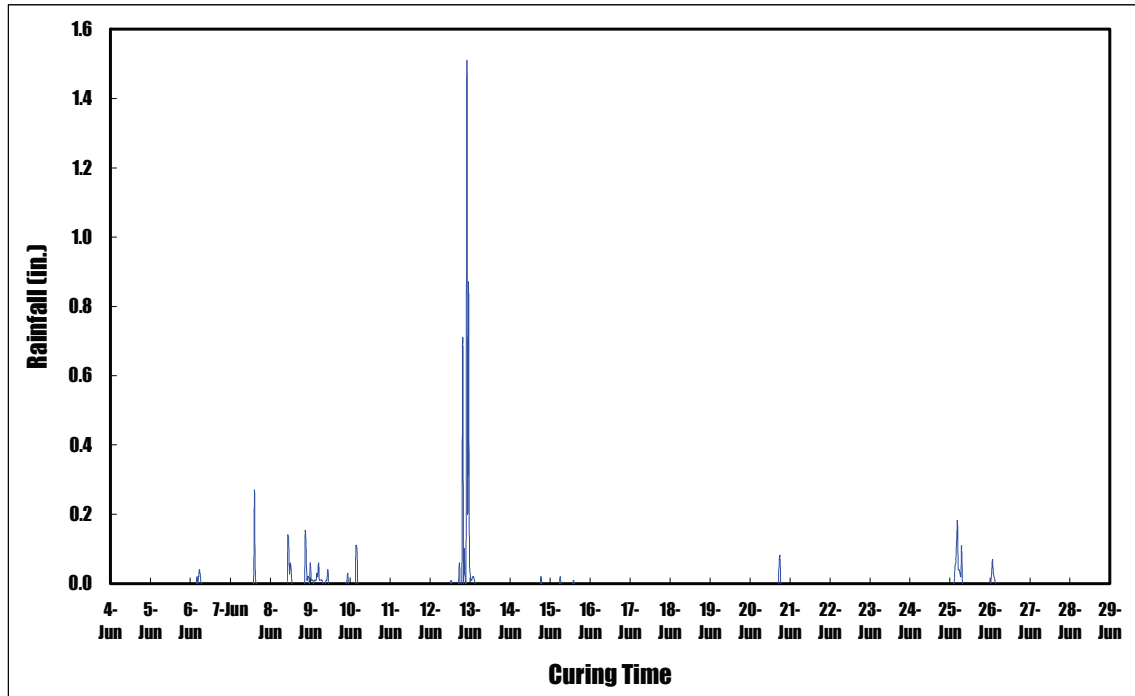
Figure 6-10. Plots of rainfalls against the curing time from weather station device
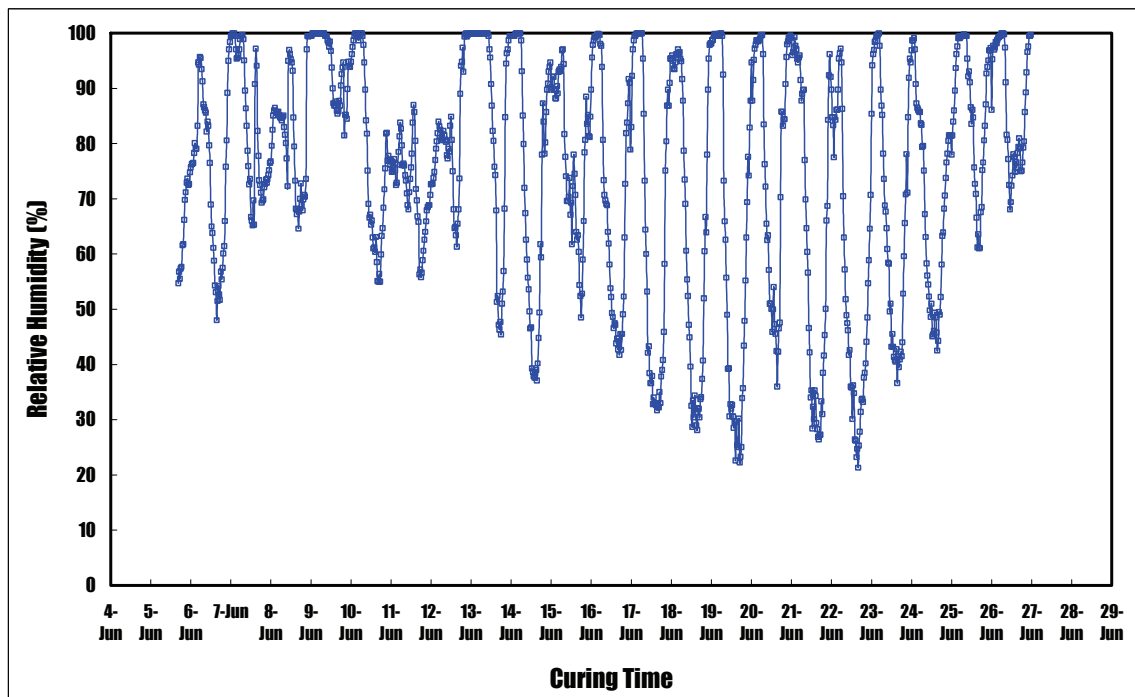
Figure 6-11. Plots of humidity against the curing time from weather station device
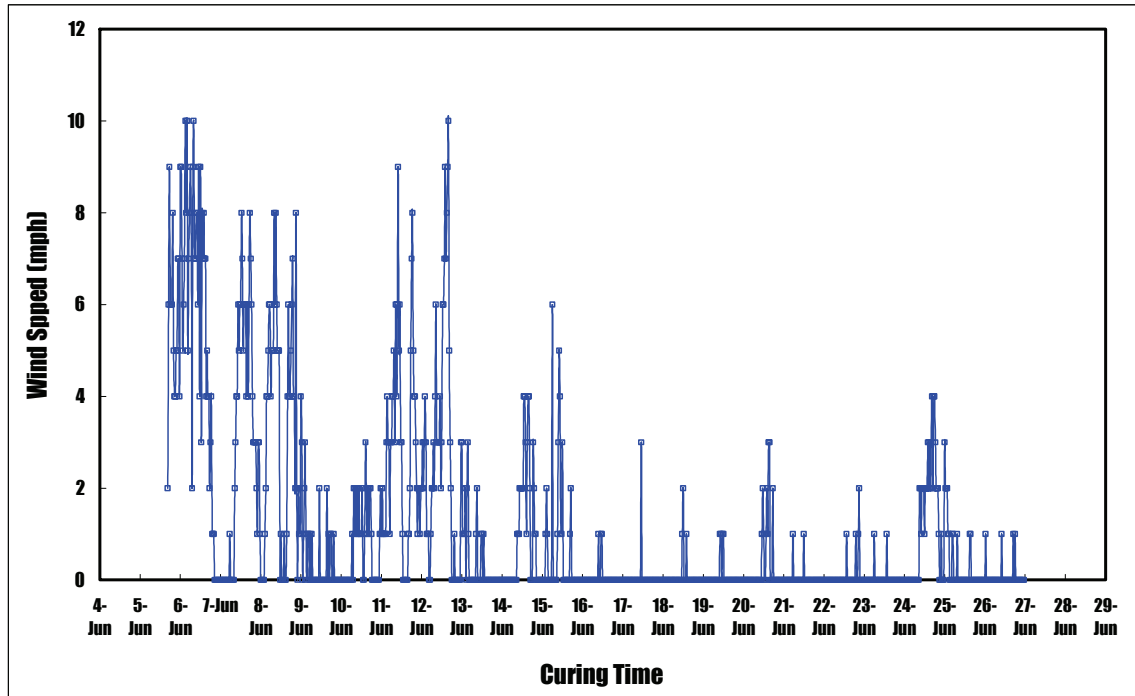
Figure 6-12. Plots of wind speed against the curing time from weather station device
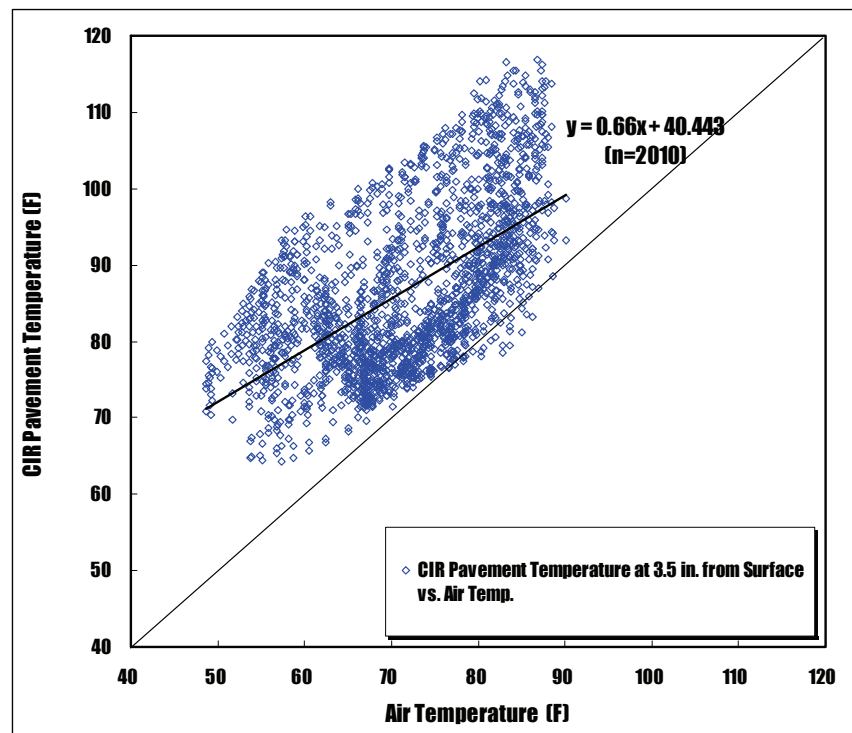
Figure 6-13. Plots of temperature from two sensors embedded in the CIR-CSS-1-emulsion layer against air temperature from weather station device

As shown in Figure 6-14, using a portable TDR device, field moisture contents were measured from ten different locations between 10:00 a.m. to 5:00 p.m. for 19 days between June 5th and 24th, 2008.   Nine measurements were made from each location and their average value was recorded for each day in Table 6-2.   Figure 6-15 shows plots of moisture contents measured between June 5th and June 24th 2008.   Figure 6-16 shows plots of field moisture content measured by a portable TDR device against field moisture content measured by a nuclear gauge.   It should be noted that the moisture contents measured using a portable TDR and a nuclear gauge represent the moisture contents between the surface and 1.5 inch to 2.0 inch from the surface and they were all above the minimum moisture content of 1.5% required for an HMA overlay.

Figure 6-17 shows comparisons of field moisture contents measured by three different methods at three locations.   As shown in Figure 6-17, moisture contents measured by a nuclear gauge at 2.0 inch consistently exhibited the lowest value followed by the portable TDR device and the capacitance moisture sensor embedded in CIR-CSS-1-emulsion layer at 3.0 inch from surface.
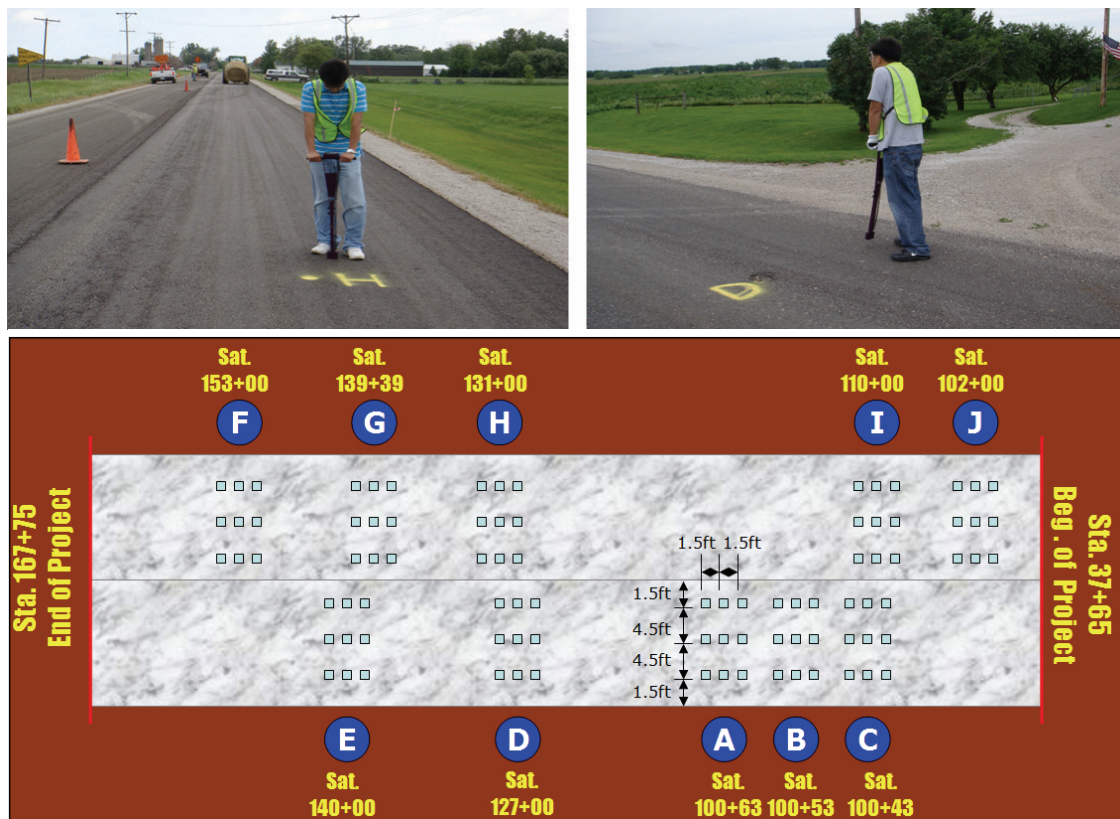
Figure 6-14. Nine moisture measurements for each location using a portable TDR

Table 6-2. Field moisture contents of CIR-CSS-1-emulsion layer

Date	Station No.									
	A 100+63	B 100+53	C 100+43	D 127+00	E 140+00	F 153+00	G 139+39	H 131+00	I 110+00	J 102+00
June 5	8.6%	8.8%	8.7%	12.2%	11.4%	-	-	-	-	-
June 6	6.0%	6.1%	6.7%	10.3%	9.0%	6.0%	11.3%	10.5%	10.1%	8.8%
June,9	7.8%	8.0%	7.8%	9.7%	13.0%	9.0%	11.2	7.9%	8.8%	8.8%
June 10	8.4%	8.3%	9.9%	10.4%	12.2%	11.2%	11.7%	7.5%	10.3%	10.3%
June 20	8.1%	7.9%	8.6%	9.1%	9.9%	9.0%	9.5%	8.1%	8.1%	8.3%
June 23	8.2%	8.2%	7.9%	8.6%	9.0%	8.5%	8.8%	7.8%	8.5%	8.8%
June 24	7.7%	7.7%	8.1%	8.2%	7.9%	7.6%	8.5%	7.5%	8.4%	8.5%
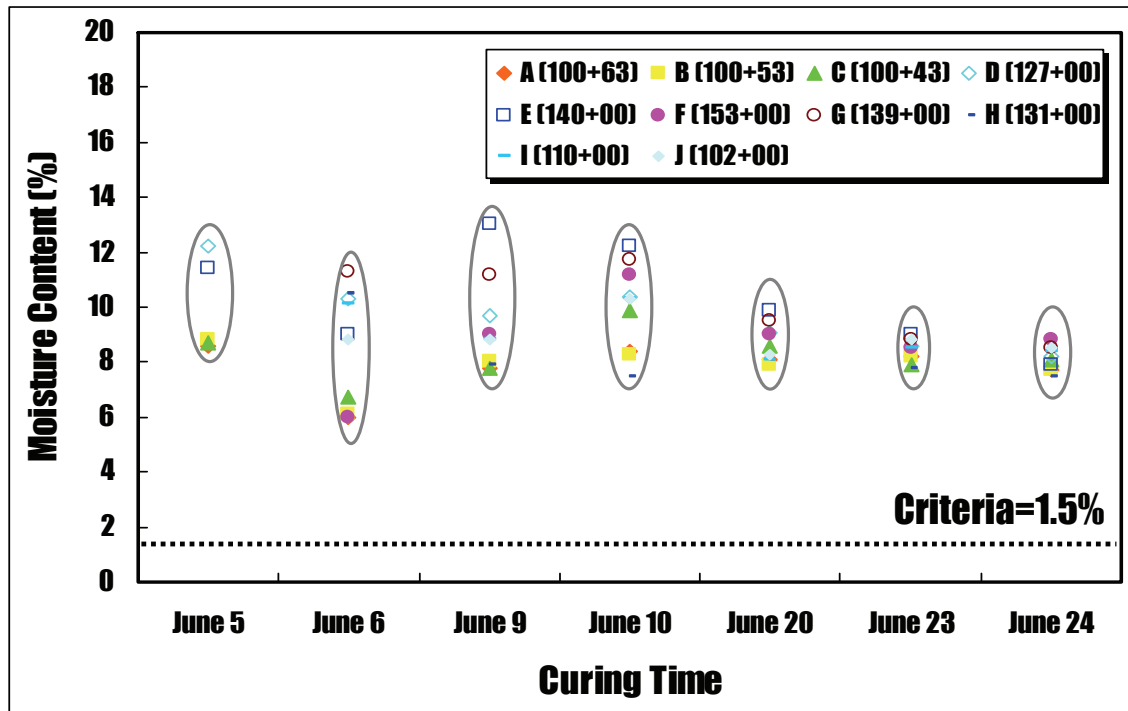
Figure 6-15. Plots of field moisture contents measured by a portable TDR

Station No.	Date Measured	TDR Device	Nuclear Gauge
100+63	June 6	6.0%	2.9%
100+53	June 6	6.1%	1.8%
100+43	June 6	6.7%	2.0%
127+00	June 6	10.3%	2.8%
140+00	June 6	9.0%	2.7%
153+00	June 9	9.0%	4.5%
139+39	June 9	11.2%	4.0%
131+00	June 9	7.9%	3.0%
110+00	June 9	8.8%	5.2%
102+00	June 9	8.8%	5.6%
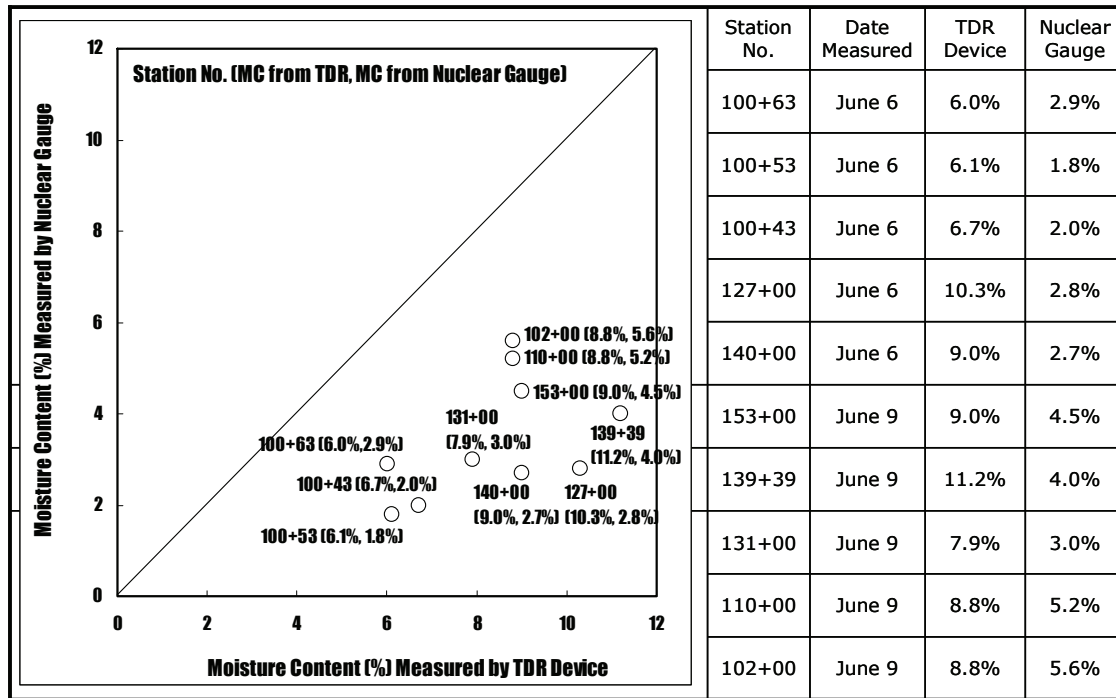
Figure 6-16. Plots of field moisture content measured by a portable TDR against field moisture content measured by a nuclear gauge
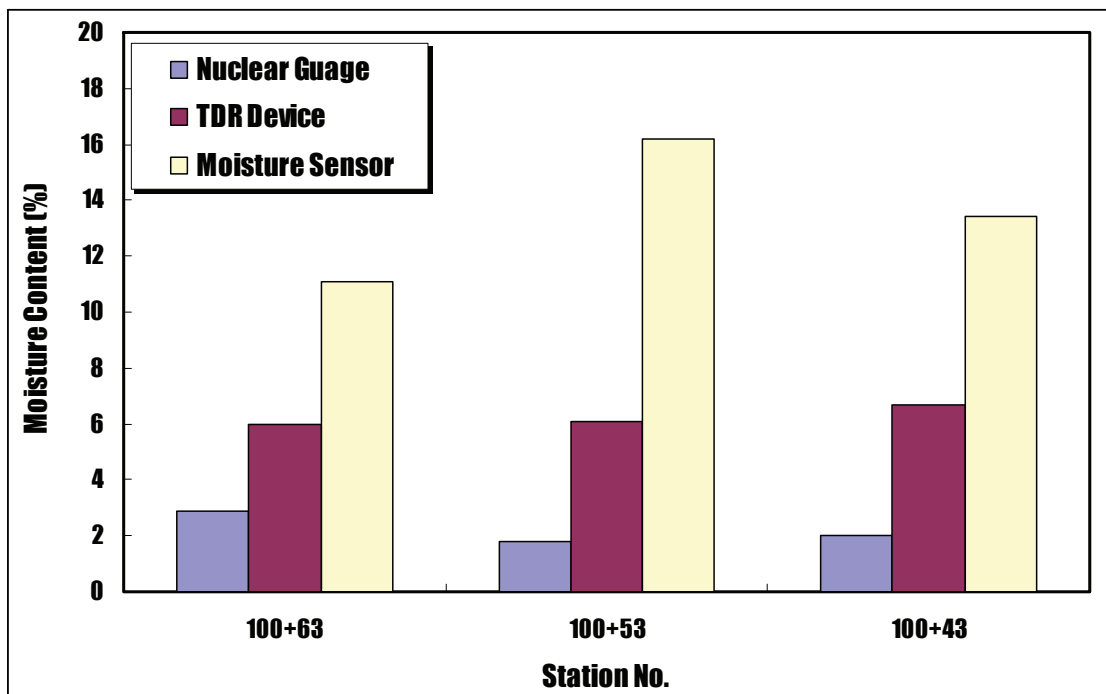
Figure 6-17. Comparisons of field moisture contents measured by three different methods at three locations

31

7. MEASUREMENT OF MOISTURE CONTENT AND TEMPERATURES USING MOISTURE AND TEMPERATURE SENSORS FROM COLD IN-PLACE RECYCLING WITH FOAMED ASPHALT LAYER

To measure the field moisture contents and temperature of CIR-foam layer, as shown in Figure 7-1, cold in-place recycling with foamed asphalt (CIR-foam) project site in Grundy County was selected.   The CIR-foam project site is located from I-175 north to County Road D 25 in Grundy County, Iowa.
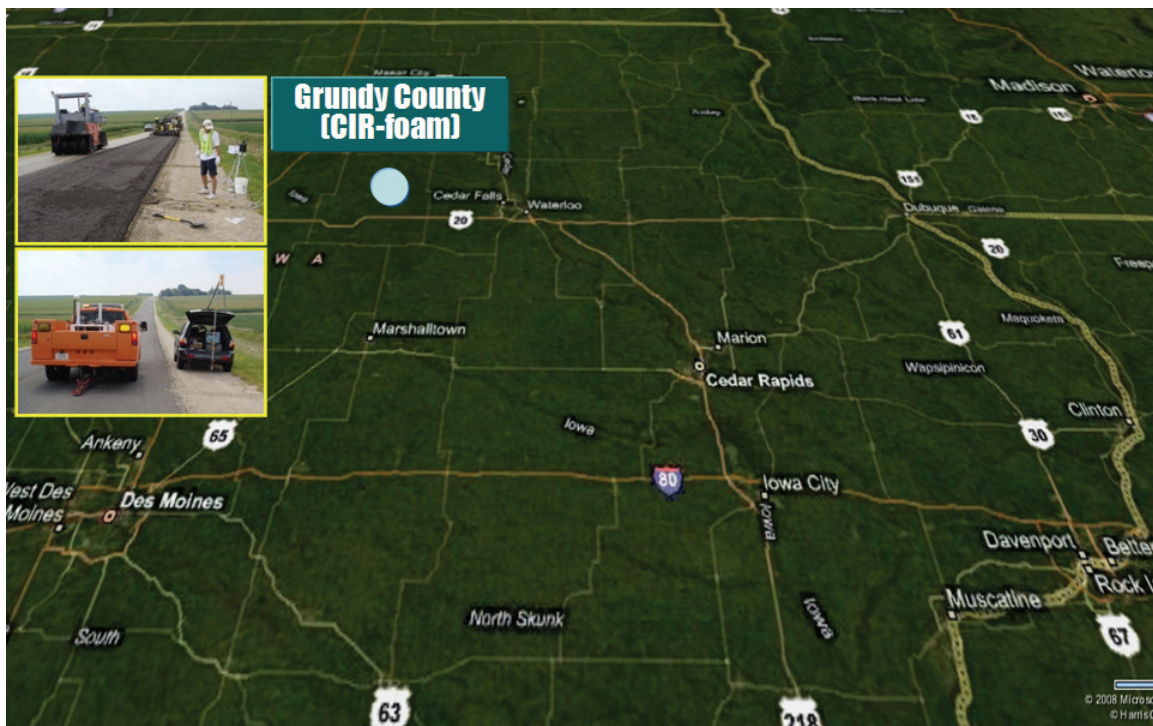
Figure 7-1. Locations of CIR-foam project sites in Grundy County

7.1 Description of CIR-foam Project in Grundy County

As shown in Figure 7-2, 6.5-mile section of County Road T 55 was rehabilitated from I-175 north to County Road D using the CIR-foam process starting on July 31, 2008.   As shown in Figure 7-3 (a), the top 3.5 inches of the existing 9-inch thick Type B HMA layer were milled and mixed with foamed asphalt to produce 3.5-inch thick CIR-foam layer. Upon completion of tack coating process on top of CIR-foam layer, 1.5-inch thick HMA

intermediate course was overlaid on August 22nd, 2008 (Figure 7-3 (c)) followed by 1.5-inch thick HMA wearing course overlaid on September 1st, 2008.

Figure 7-2. Cross section of CIR-foam project in Grundy County

(a) CIR-foam process

(b) Curing process

(c) Intermediate HMA overlay process

Figure 7-3. Pictures of CIR-foam, curing, and HMA overlay processes

7.2 Survey of Existing Pavement Condition

6.5-mile section of County Road T 55 had been surveyed before it was rehabilitated.   As shown in Figure 7-4, a large amount of traverse cracks and longitudinal cracks were observed. Minor wheel-path rutting and raveling were also observed.

Figure 7-4. Pictures of surface conditions of the existing pavement

7.3 Collection of CIR-foam Mixture

To measure the moisture content of CIR-foam field mixtures in the laboratory, as shown in Figure 7-5, CIR-foam mixtures were collected from three different locations between 11:30 a.m. to 1:00 p.m. on July 31st, 2008.   Table 7-1 summarizes the laboratory moisture contents of CIR-foam field mixtures that were collected from two locations. The average moisture content of 3.3% measured at University of Iowa was lower than the 3.9% measured by a contractor.

Figure 7-5. Locations of collecting CIR-foam field mixtures

Table 7-1. Laboratory moisture content of CIR-foam field mixtures

	University of Iowa				Contractor
Station No.	# 1	# 2	# 3	Average	Average
388+00	3.8%	3.2%	3.4%	3.5%	3.9%
382+00	2.9%	3.1%	3.4%	3.1%	
			Total Average	3.3%	3.9%

7.4 Measurement of Field Moisture Content and Temperature using Moisture and Temperature Sensors

To monitor actual moisture contents of the CIR-foam layer in the field, as shown in Figure 7-6, two ECH$_2$O moisture sensors and one temperature sensor were installed at the bottom and one ECH$_2$O moisture sensor and one temperature sensor were installed in the middle of the CIR-foam layer.   A weather station was also installed to collect air temperature, humidity, rainfall and wind speed.   Figure 7-7, Figure 7-8, Figure 7-9, Figure 7-10, Figure 7-11 show plots of moisture contents, temperatures, rainfall, humidity, and wind speed, respectively, measured during a curing time of 22 days when eleven rainfalls with a total amount of 1.54 inch had occurred.   The moisture contents before the intermediate HMA overlay were measured at 12.1% from sensor A' in the middle of the CIR-foam layer, 7.2% from sensor A at the bottom, and 14.5% from sensor B at the bottom.   Despite the actual moisture contents of CIR-foam layer remaining above 1.5%, the intermediate HMA overlay was constructed after 22 days of curing. Figure 7-12 shows plots of temperature from three sensors embedded in the CIR-foam layer against air temperature from weather station device.   As shown in Figure 7-12, temperature of CIR-foam layer was higher than air temperature.
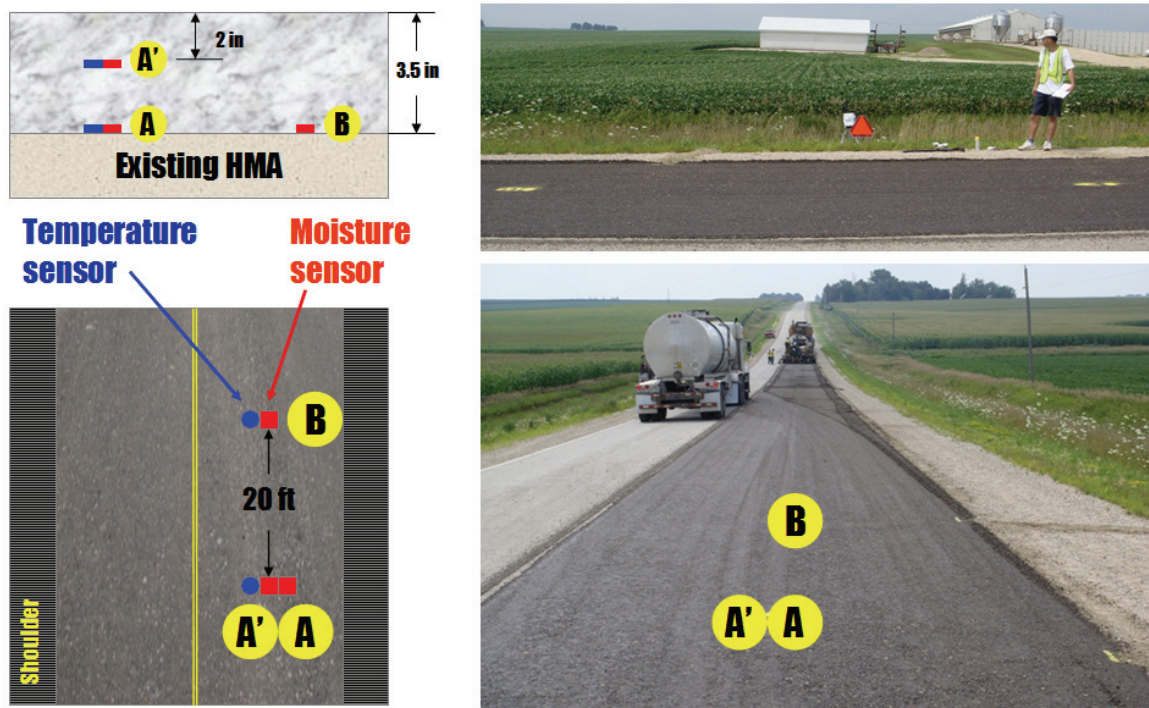
Figure 7-6. Embedded moisture and temperature sensors installed at a midpoint and a bottom of the CIR layer

37
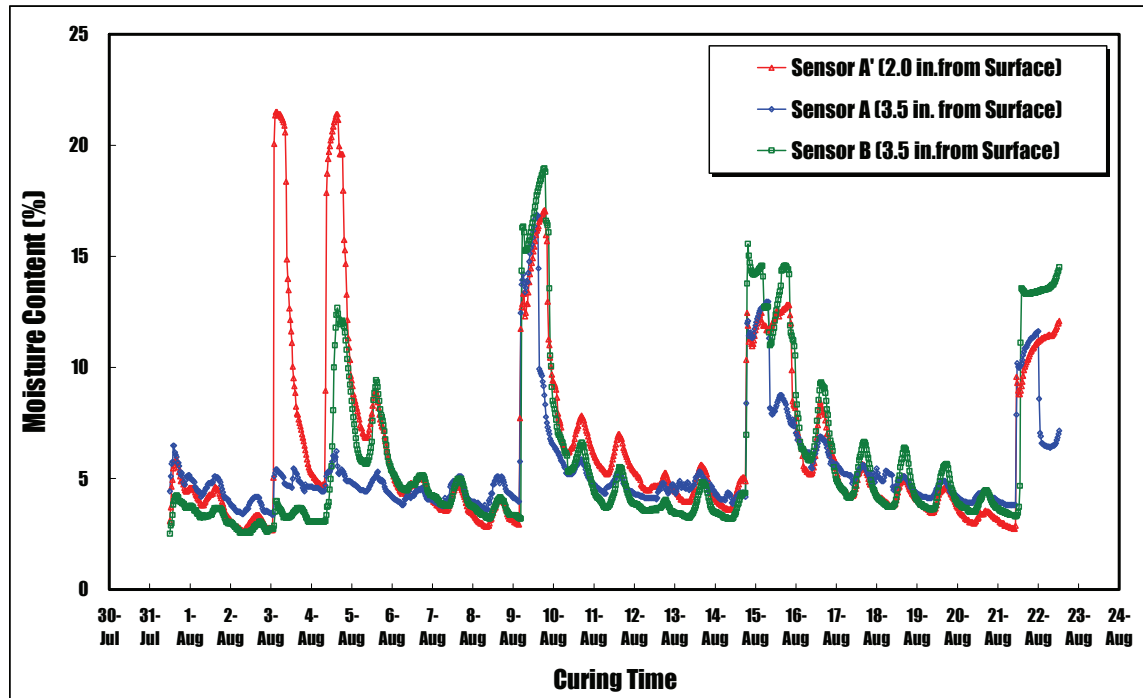
Figure 7-7. Plots of moisture contents against the curing time from three sensors embedded in the CIR-foam layer
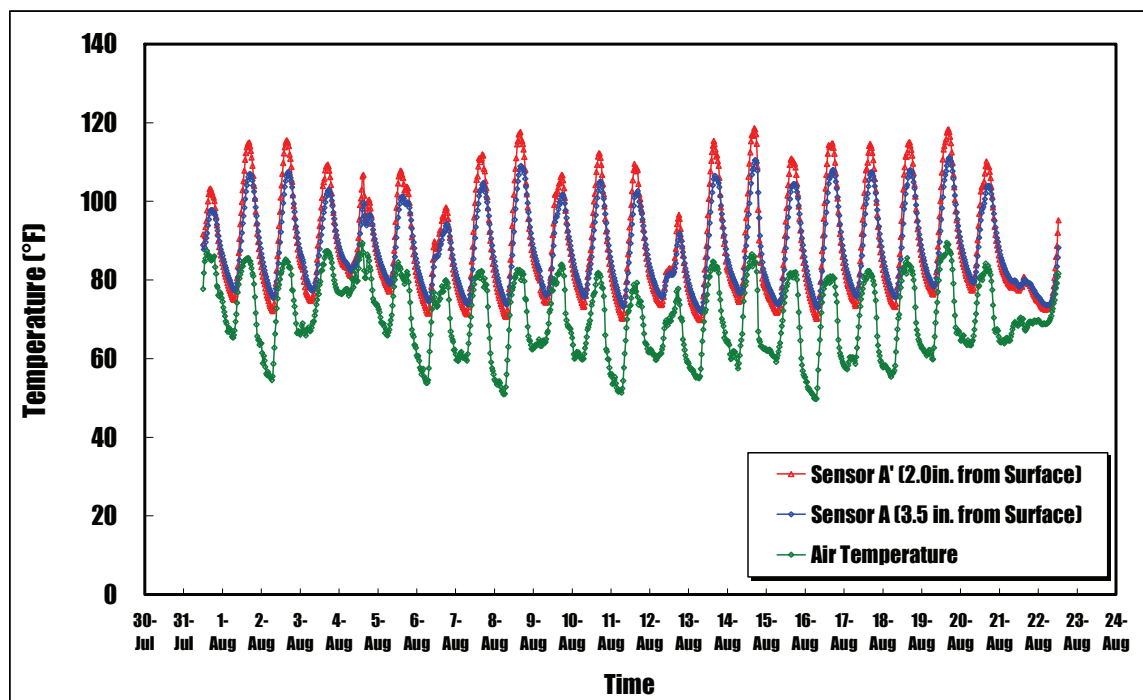
Figure 7-8. Plots of temperature against the curing time from two sensors embedded in the CIR-foam layer and air temperature from weather station device

38
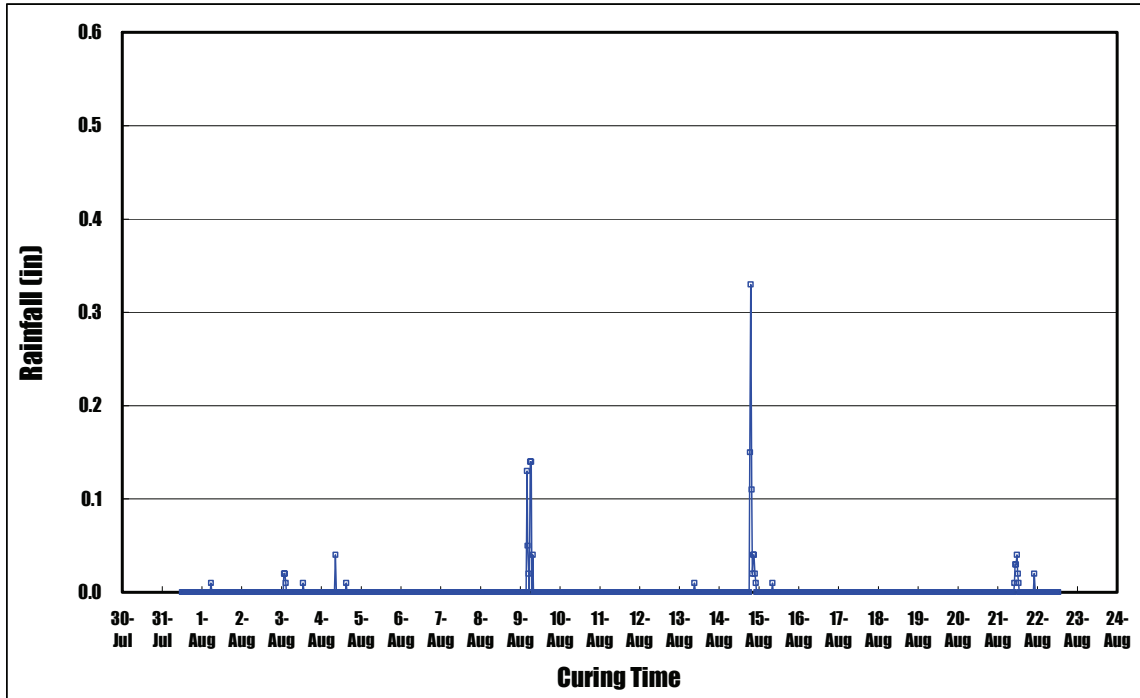
Figure 7-9. Plots of rainfalls against the curing time from weather station device
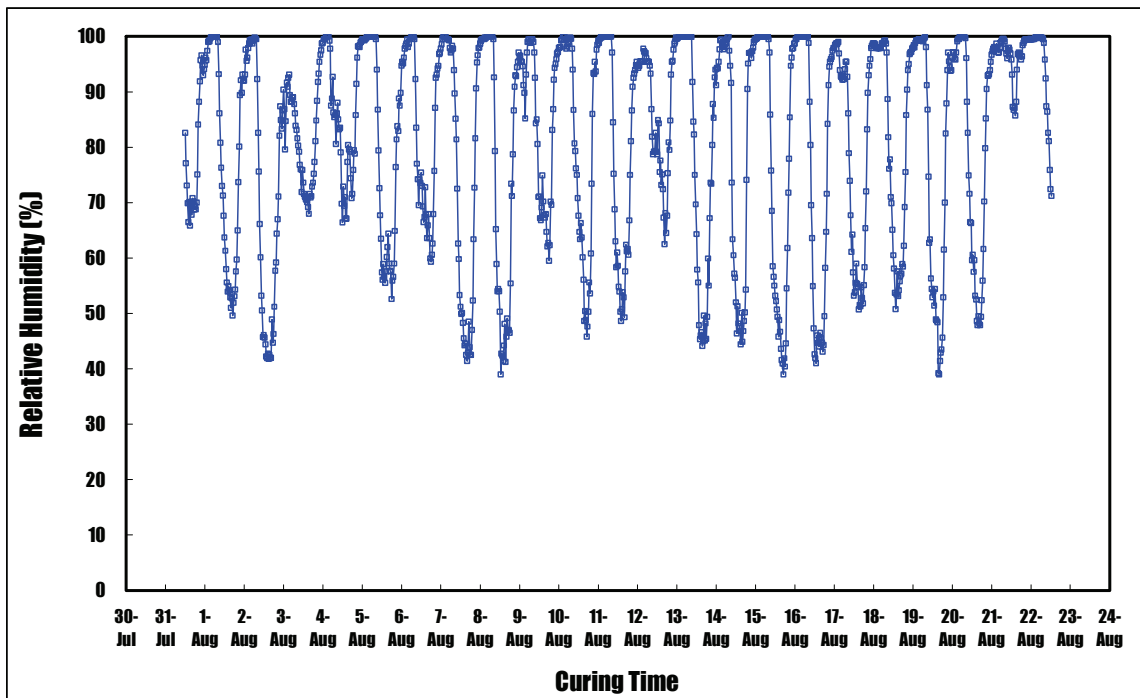
Figure 7-10. Plots of humidity against the curing time from weather station device

39
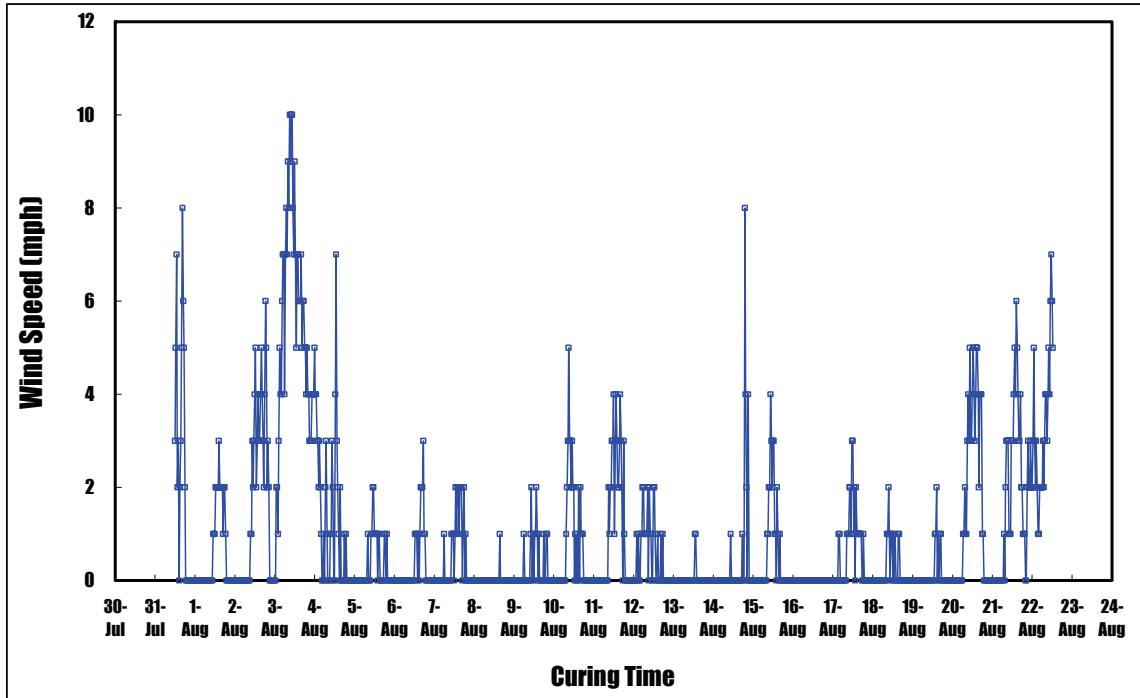
Figure 7-11. Plots of wind speed against the curing time from weather station device
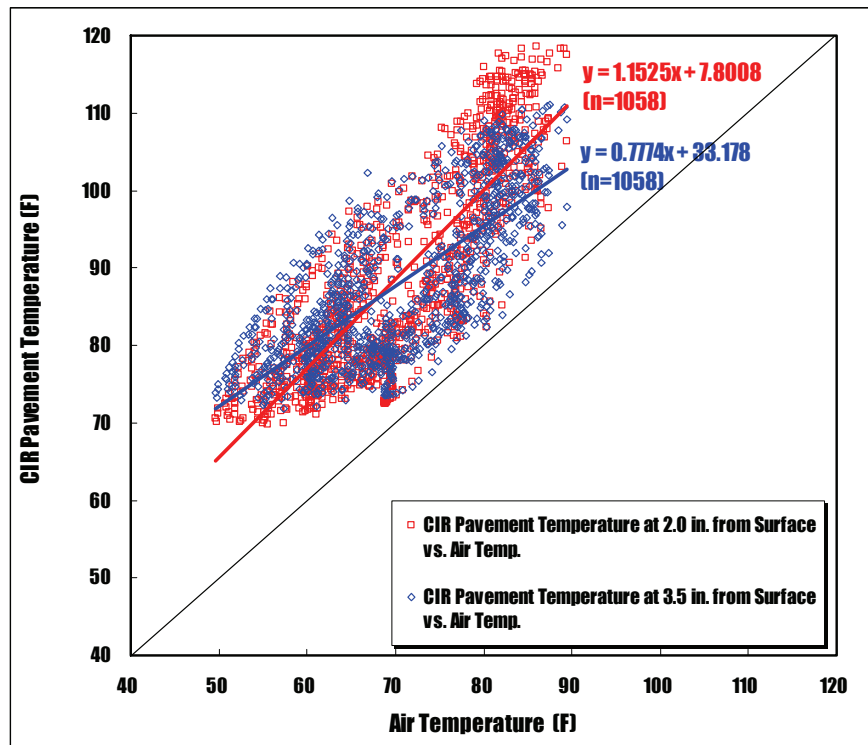
Figure 7-12. Plots of temperature from two sensors embedded in the CIR-foam layer against air temperature from weather station device

As shown in Figure 7-13, using a portable TDR device, field moisture contents were measured from three different locations between 11:00 a.m. to 12:30 p.m. for 19 days between July 31st and August 22nd, 2008.   As shown in Figure 7-13, nine measurements were made from each location and the average value was recorded for each day in Table 7-2.   Figure 7-14 shows plots of moisture contents measured between July 31st and August 22nd, 2008.   Figure 7-15 shows plots of field moisture content measured by a potable TDR device against field moisture content measured by a nuclear gauge.   It should be noted that the moisture contents measured using a portable TDR and a nuclear gauge represent the moisture contents between the surface and 1.5 inch to 2.0 inch from the surface and they were above the minimum moisture content of 1.5% required before an HMA overlay.

Figure 7-16 shows comparisons of field moisture contents measured by three different methods at three locations.   As shown in Figure 7-16, moisture content measured by a nuclear gauge at 2.0 inch exhibited the lowest value followed by the capacitance moisture sensor and the portable TDR device.

Figure 7-13. Nine moisture measurements for each location using a portable TDR

Table 7-2. Field moisture contents of CIR-foam layer using a portable TDR

Date	Station No.		
	A (380+80)	B (380+60)	C (382+00)
July 31	8.5%	8.5%	12.3%
August 1	7.1%	6.8%	10.7%
August 6	7.4%	6.7%	9.4%
August 12	8.6%	7.2%	8.5%
August 18	7.7%	7.4%	8.2%
August 20	6.9%	6.7%	7.8%
August 22	7.8%	6.5%	9.1%
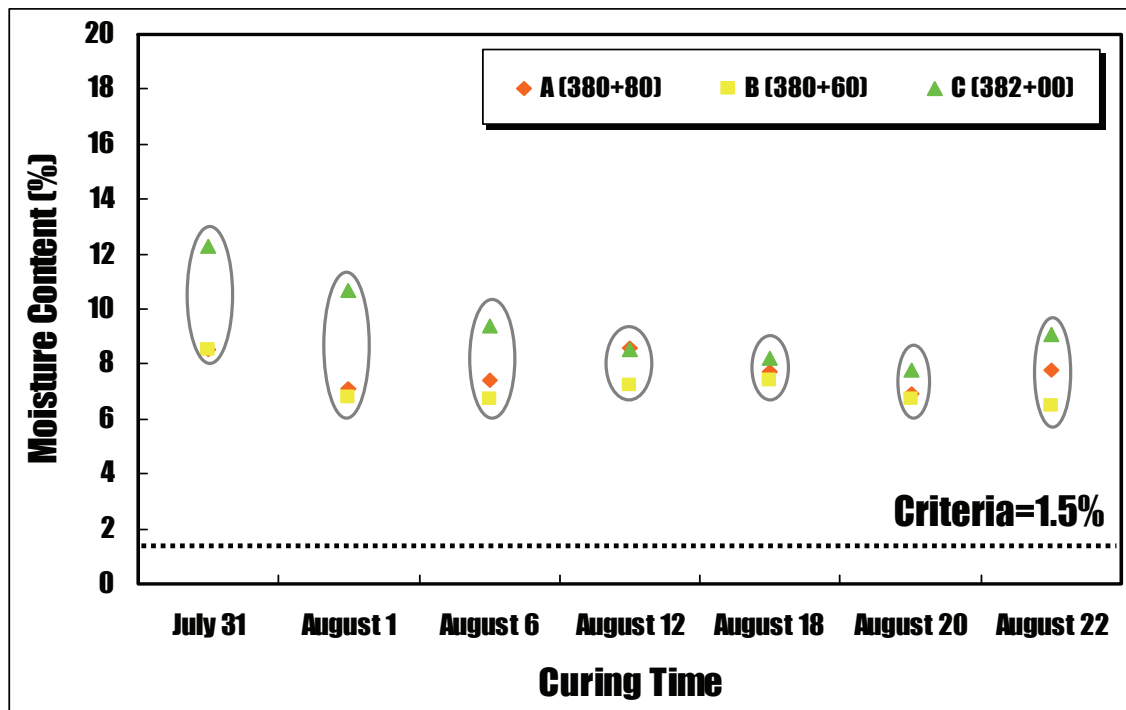
Figure 7-14. Plots of field moisture contents measured by a portable TDR

Station No.	Date Measured	TDR Device	Nuclear Gauge
380+80	August 1	7.1%	2.6%
380+60	August 1	6.8%	1.6%
382+00	August 1	10.7%	3.8%
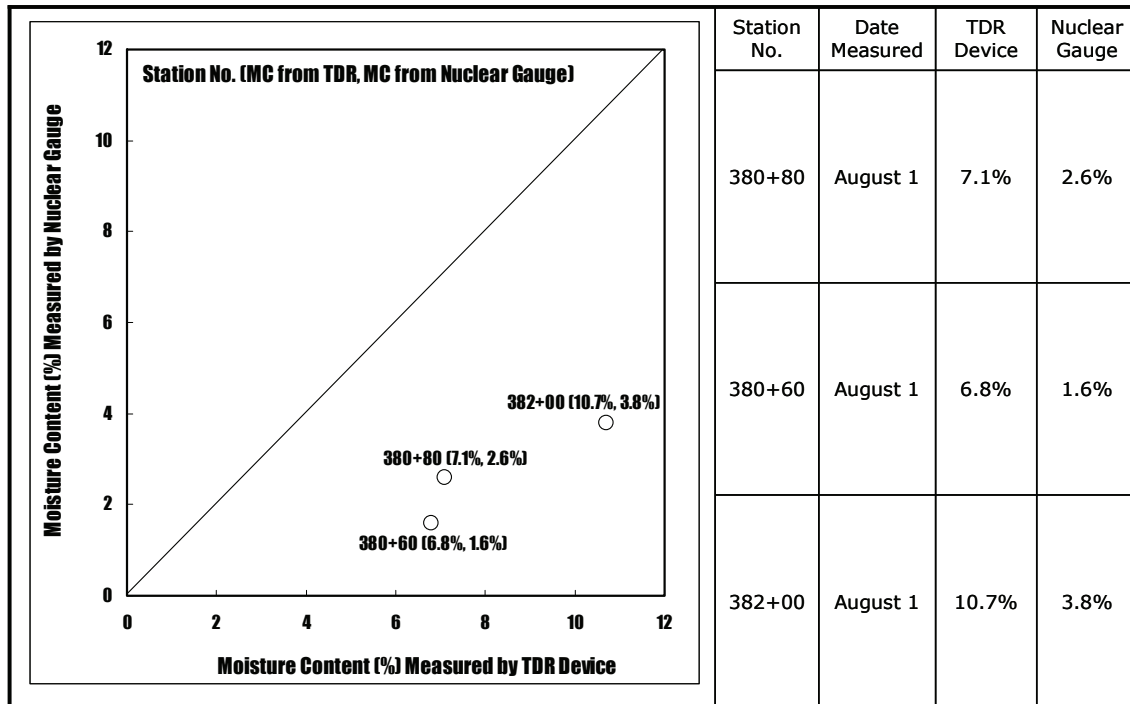
Figure 7-15. Plots of field moisture content measured by a potable TDR against field moisture content measured by a nuclear gauge
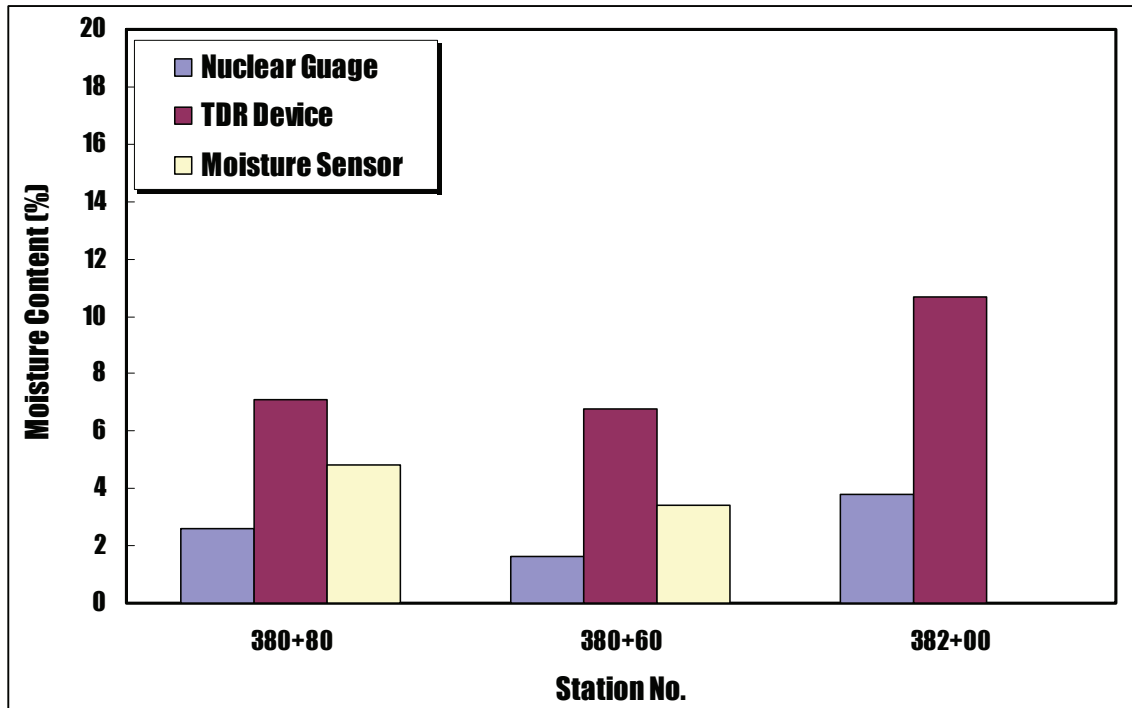
Figure 7-16. Comparisons of field moisture contents measured by three different methods at three locations

7.5. Measurement of Modulus and Stiffness of CIR Layer

The modulus and stiffness of the CIR-foam layer was measured using falling weight deflectometer (FWD) and geo-gauge, respectively, during the curing time. As shown in Figure 7-17, the modulus and stiffness were measured at three different locations: (1) A (Sensor A' and A), (2) B (Sensor B) and (3) C (no sensor).
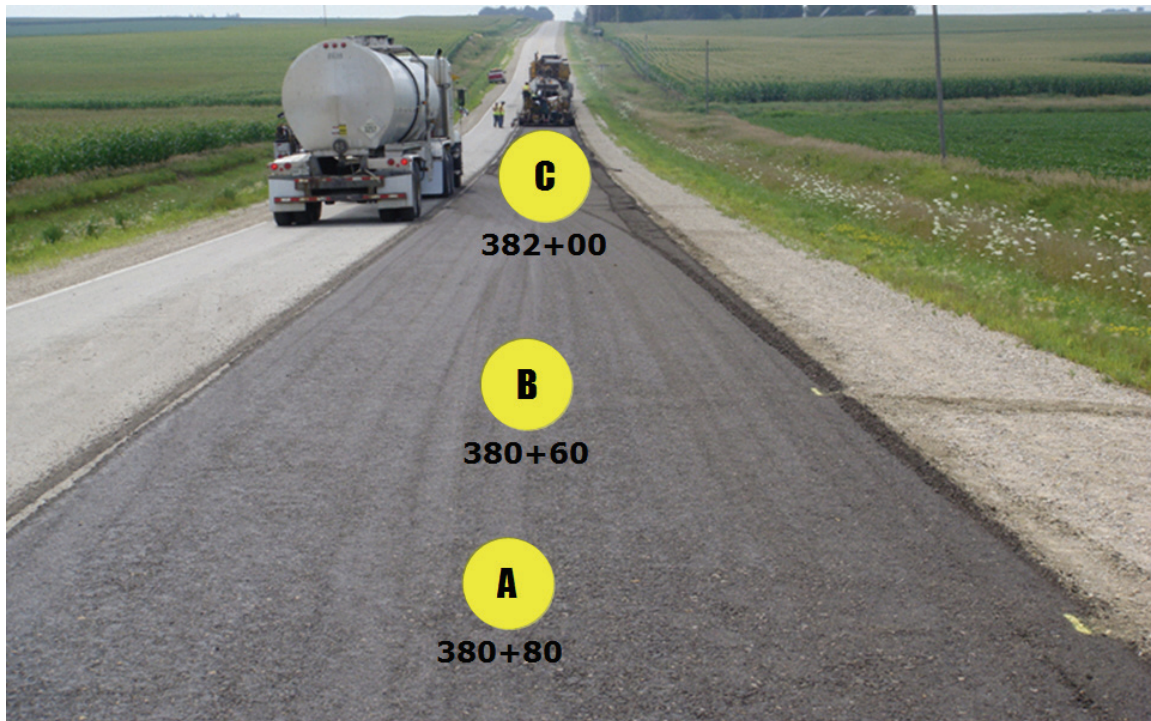
Figure 7-17. Location of three spots for measuring modulus and stiffness

7.5.1 Modulus Measurements using FWD

As shown in Figure 7-18, FWD was used to measure deflections of CIR-foam layer. As shown in Figure 7-19, modulus values were back-calculated from the deflection measured four times between August 5th and August 20th, 2008 from three locations (all deflection measurements were made between 12:10 p.m. to 1:00 p.m.). As expected, the modulus value of CIR-foam layer increased as the curing time increased. It should be noted that the modulus decreased due to the rainfalls between August 13th and 15th, 2008.

Figure 7-18. Measuring modulus of the CIR-foam layer using FWD
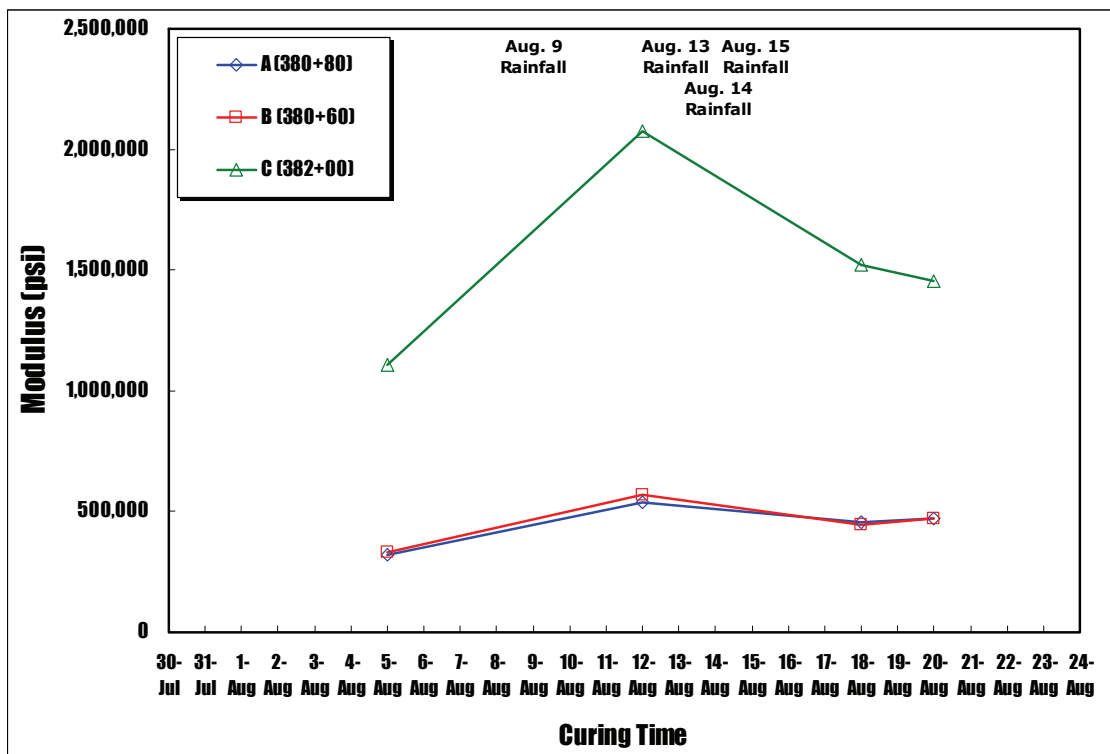
Figure 7-19. Plots of modulus against curing time from three locations in the CIR-foam layer

45

7.5.2 Stiffness Measurements using Geo-gauge

As shown in Figure 7-20, the geo-gauge was used to measure the stiffness of CIR-foam layer.   The geo-gauge is a portable device capable of measuring the in-situ stiffness of soil.   As shown in Figure 7-21, stiffness was measured seven times between July 31st and August 22nd, 2008 from three locations (all stiffness measurements were made between 11:15 a.m. to 1:40 p.m.).   As expected, the stiffness of CIR-foam layer increased as curing time increased.   However, there was no correlation between the stiffness and the moisture content.   For example, although the moisture content increased significantly to 14.5% after the rainfall but the stiffness remained high at 29.1 MN/m.   Despite the moisture content remaining above 1.5% during the curing period of 22 days, the stiffness of the CIR-foam layer increased steadily for the first 12 days and remained relatively high for the next 10 days after rainfalls on August 13th, 14th, 15th and 21st, 2008.   This indicates that the layer stiffness would be affected by the pavement temperature more than moisture content. Therefore, to be conservative, the stiffness should be measured at the highest temperature of the day that could handle an overlay. If the weather gets hotter after the CIR construction, it could either increase the stiffness due to the accelerated curing or decrease the stiffness due to a high temperature.

Figure 7-22 shows plots of stiffness measured by geo-gauge against modulus measured by FWD at three different locations on August 12th and August 18th, 2008.   Figure 7-23 shows plots of stiffness measured by geo-gauge against density measured by a nuclear gauge at three different locations on August 1st, 2008.   As shown in Figure 7-22 and Figure 7-23, the stiffness seemed to increase as the modulus and density increased.   It should be explored if the stiffness may be a more appropriate measure than the moisture content for determining an optimum timing for an overlay.

Figure 7-20. Measuring stiffness of the CIR-foam layer using geo-gauge
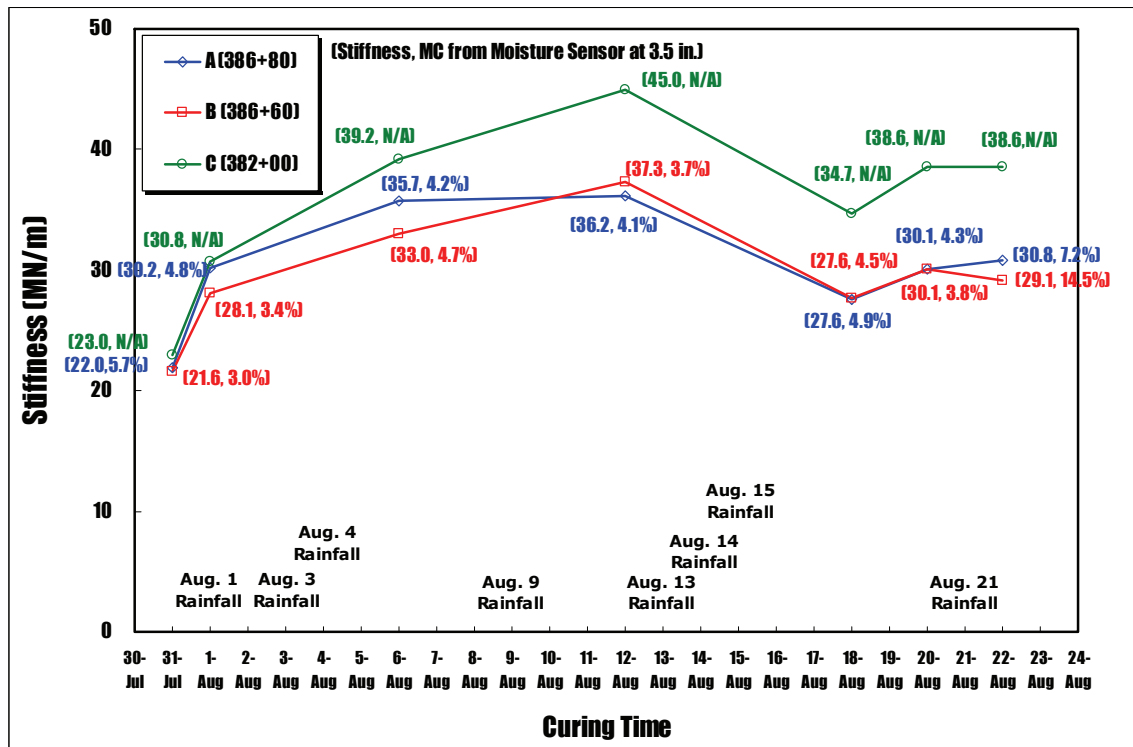
Figure 7-21. Plots of stiffness against the curing time from three locations in the CIR-foam layer

47
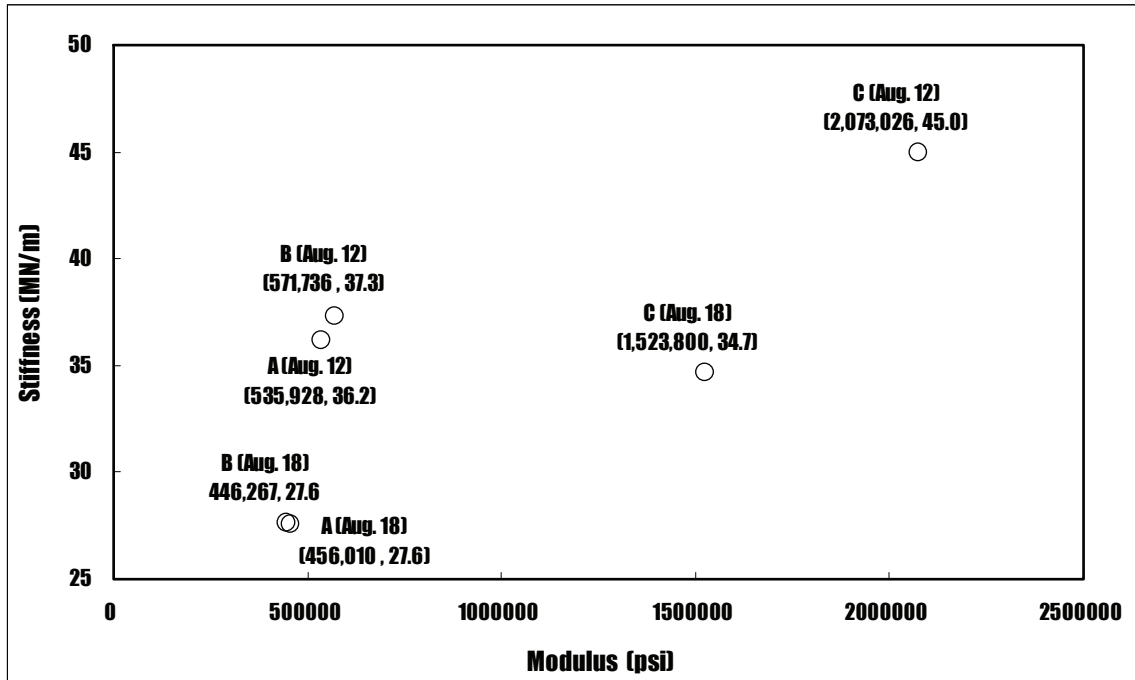
Figure 7-22. Plots of stiffness measured by geo-gauge against modulus measured by FWD at three different locations
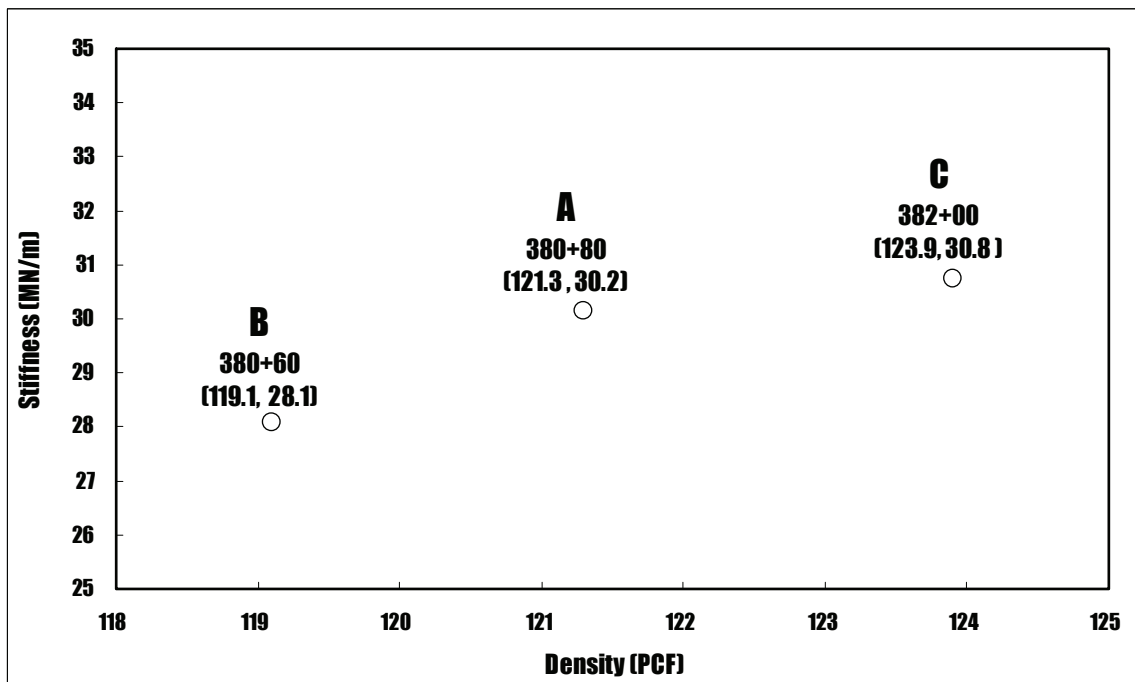
Figure 7-23. Plots of stiffness measured by geo-gauge against density measured by a nuclear gauge at three different locations

8. DEVELOPMENT OF MOISTURE LOSS INDEX FOR CIR LAYER

To develop moisture loss index for CIR layer, as shown in Figure 8-1, the actual moisture contents of CIR layer were measured by a portable TDR device and ECH_2O moisture sensors in three CIR project sites in 2008.

Figure 8-1. Locations of three CIR project sites in Iowa

8.1 CIR-foam Project Site in Cedar County

To predict the moisture condition in the CIR-foam layer in Cedar County, a moisture loss index was developed as a function of initial moisture content, cumulative air temperature, cumulative humidity and the cumulative wind speed as follows:

$$\triangle MC/hr = a_1 + a_2\ I_{MC} + a_3\ C_{Temp}/hr + a_4\ C_{\ humidity}\ /hr + a_5\ C_{windspeed}/hr$$

Where,

$\triangle MC$ = change in moisture contents between two measurements

h = time between two measurements in hours

I_{MC} = the actual moisture contents of CIR layer measured in the field using a portable TDR device

C_{Temp} = cumulative air temperature (˚C) between moisture measurements

$C_{humidity}$ = cumulative humidity (%) between moisture measurements

$C_{windspeed}$ = cumulative wind speed (km/h) between moisture measurements

$a_1,\ a_{2,}\ a_3,\ a_4,\ a_5$ = multiple linear regression coefficients

Table 8-1 and Table 8-2 summarize fifty-six sets of measurements from the field and weather information.   As highlighted in Table 8-1 and Table 8-2, negative or very small moisture changes were removed from the further analysis because they might have been affected by the precipitation.   Consequently, twenty-one sets of data points were used for developing the moisture loss index.   As shown in the regression equation below, Δmoisture content per hour in CIR layer can be predicted as a function of the initial moisture content, cumulative temperature per hour, and humidity per hour and wind speed per hour for the CIR-foam project site on County Road X 30, Cedar County, Iowa.

$$\Delta MC/hr = -0.139 + 0.0215\ I_{MC} + 0.00957\ C_{Temp}/hr + 0.000963\ C_{humidity}/hr$$
$$- 0.00669\ C_{windspeed}/hr\ (R\text{-square} = 66.1\%)$$

Table 8-1. Summary of Δmoisture content/hour, initial moisture content, cumulative temperature/hour, humidity/hour and wind speed/hour

Station No.	Curing Period	ΔMoisture Content /hour	Initial Moisture Content	C_{Temp} /hour	$C_{Humidity}$ /hour	$C_{Windspeed}$ /hour
140+00	05/05~05/06	0.000	2.610	16.991	50.217	8.306
	05/06~05/07	-0.011	2.602	25.929	102.353	21.092
	05/07(am)~ 05/07(pm)	0.110	3.44	20.08	64.83	15.18
	05/10~05/11	- 0.055	2.848	12.232	77.640	30.172
	05/11~05/12	0.028	4.213	10.579	62.708	12.902
	05/12~05/13	- 0.021	3.553	15.817	60.340	19.182
	05/13~05/14	0.037	4.056	13.686	55.605	14.397
	05/14~05/15	0.024	3.239	14.282	17.727	8.946
95+00	05/06(am)~ 05/06(pm)	0.070	3.39	28.41	47.86	25.68
	05/06~05/07	-0.030	2.87	18.81	80.47	15.95
	05/07~05/09	0.010	3.45	13.79	52.77	11.87
	05/09~05/10	- 0.040	3.034	13.618	70.227	6.415
	05/10~05/11	- 0.033	3.914	12.232	77.640	30.172
	05/11~05/12	0.031	4.728	10.579	62.708	12.902
	05/12~05/13	- 0.028	3.973	15.817	60.340	19.182
	05/13~05/14	0.020	4.625	13.686	55.605	14.397
	05/14~05/15	0.045	4.180	14.282	17.727	8.946
45+00	05/06~05/07	- 0.029	2.681	18.806	80.471	15.951
	05/07(am)~ 05/07(pm)	- 0.006	3.177	20.083	64.833	15.181
	05/07~05/09	- 0.003	3.210	13.788	52.771	11.872
	05/09~05/10	0.000	3.342	13.618	70.227	6.415
	05/10~05/11	- 0.061	3.342	12.232	77.640	30.172
	05/11~05/12	0.031	4.856	10.579	62.708	12.902
	05/12~05/13	- 0.020	4.124	15.817	60.340	19.182
	05/13~05/14	0.058	4.586	13.686	55.605	14.397
	05/14~05/15	0.007	3.304	14.282	17.727	8.946
9+50	05/07(am)~ 05/07(pm)	- 0.048	1.887	20.083	64.833	15.181
	05/07~05/09	0.009	2.176	13.788	52.771	11.872
	05/09~05/10	- 0.030	1.726	13.618	70.227	6.415
	05/10~05/11	- 0.039	2.381	12.232	77.640	30.172
	05/11~05/12	0.009	3.347	10.579	62.708	12.902
	05/12~05/13	0.005	3.130	15.817	60.340	19.182
	05/13~05/14	0.025	3.019	13.686	55.605	14.397
	05/14~05/15	0.024	2.464	14.282	17.727	8.946

Table 8-2. Summary of Δmoisture content/hour, initial moisture content, cumulative temperature/hour, humidiy/hour and wind speed/hour

Station No.	Curing Period	ΔMoisture Content /hour	Initial Moisture Content	C_{Temp} /hour	$C_{Humidity}$ /hour	$C_{Windspeed}$ /hour
43+50	05/07~05/08	0.009	2.340	13.915	52.683	15.910
	05/08~05/09	0.013	2.120	13.763	52.946	8.154
	05/09~05/10	- 0.031	1.811	13.618	70.227	6.415
	05/10~05/11	- 0.074	2.500	12.232	77.640	30.172
	05/11~05/12	0.044	4.344	10.579	62.708	12.902
	05/12~05/13	- 0.015	3.282	15.817	60.340	19.182
	05/13~05/14	0.030	3.628	13.686	55.605	14.397
	05/14~05/15	0.015	2.957	14.282	17.727	8.946
54+00	05/08~05/09	- 0.003	2.305	13.763	52.946	8.154
	05/09~05/10	- 0.013	2.386	13.618	70.227	6.415
	05/10~05/11	- 0.080	2.681	12.232	77.640	30.172
	05/11~05/12	0.043	4.680	10.579	62.708	12.902
	05/12~05/13	- 0.016	3.648	15.817	60.340	19.182
	05/13~05/14	0.031	4.024	13.686	55.605	14.397
	05/14~05/15	0.026	3.326	14.282	17.727	8.946
125+00	05/08~05/09	0.006	2.848	13.763	52.946	8.154
	05/09~05/10	- 0.001	2.704	13.618	70.227	6.415
	05/10~05/11	- 0.122	2.733	12.232	77.640	30.172
	05/11~05/12	0.070	5.778	10.579	62.708	12.902
	05/12~05/13	- 0.014	4.088	15.817	60.340	19.182
	05/13~05/14	0.038	4.411	13.686	55.605	14.397
	05/14~05/15	0.009	3.558	14.282	17.727	8.946

8.2 CIR-emulsion Project Site in Scott County

Based on the individual correlation analysis, it was discovered that there was very little correlation between the moisture loss and either wind speed and humidity. Therefore, to predict the moisture condition in the CIR-emulsion layer in Scott County, a moisture loss index was developed as a function of the initial moisture content and the cumulative pavement temperature per hour as follows:

$$\triangle MC/hr = a_1 + a_2\ I_{MC} + a_3\ C_{Temp}/hr$$

Where,

I_{MC} = the actual moisture contents of CIR layer measured in the field using the embedded ECH_2O moisture sensor

C_{Temp} = cumulative pavement temperature (˚F) between moisture measurements

$a_1,\ a_2,\ a_3$ = multiple linear regression coefficients

Table 8-3 summarizes twenty-four sets at sensor A, twenty-three sets at Sensor B, and twenty-three sets at sensor C between rainfalls.

As highlighted in Table 8-3, the data sets with the initial moisture content above 14% were removed from the further analysis because they are excessive moisture conditions which are beyond the moisture loss modeling range for CIR-emulsion. Consequently, ten sets of data points at sensor A, six sets of data points at sensor B, and nineteen sets of data points at sensor C were used for developing the moisture loss index.

As shown in the regression equation for each of three locations below, Δmoisture content/hour in CIR-emulsion layer can be predicted as a function of the initial moisture content and the cumulative pavement temperature per hour for the CIR-emulsion project site on County Road Y-40, Scott County, Iowa.

Sensor A: $\Delta MC/hr = 4.70 + 0.175\ I_{MC} - 0.0701\ C_{Temp}/hr$ (R-square = 57.3%)
Sensor B: $\Delta MC/hr = -0.545 - 0.0152\ I_{MC} + 0.0102\ C_{Temp}/hr$ (R-square = 75.5%)
Sensor C: $\Delta MC/hr = 4.19 - 0.0370\ I_{MC} - 0.0409\ C_{Temp}/hr$ (R-square = 20.7%)

Overall, R-square values are relatively small and these equations may not be reliable for predicting moisture level in a typical CIR-emulsion layer because it was constructed on top of concrete pavement.

Table 8-3. Summary of Δmoisture content/hour, initial moisture content, and cumulative pavement temperature/hour for CIR-emulsion project in Scott County

	Sensor No							
A (100+63)			B (100+53)			C (100+43)		
ΔMC /hour	Initial MC	C$_{Temp}$ /hour	ΔMC /hour	Initial MC	C$_{Temp}$ /hour	ΔMC /hour	Initial MC	C$_{Temp}$ /hour
0.26	10.0	88.0	0.23	6.0	87.4	0.17	4.2	88.8
2.71	12.7	77.8	0.04	17.5	82.8	2.15	11.8	73.5
4.13	16.2	93.2	0.34	17.6	91.5	0.06	16.1	80.8
5.41	15.2	80.5	0.73	17.0	79.6	0.89	15.8	94.2
0.61	11.6	79.1	0.34	16.8	80.5	1.20	11.9	77.1
1.15	7.5	74.7	0.15	16.2	75.0	0.72	14.2	84.4
1.50	12.1	74.1	0.04	15.6	85.1	0.17	11.8	68.3
1.11	9.7	68.1	0.04	15.6	79.3	0.07	14.1	84.4
0.79	15.8	80.8	0.45	15.7	78.9	0.04	13.1	81.1
2.06	16.1	84.4	0.11	15.3	80.0	0.05	13.2	79.4
0.05	14.8	80.1	0.09	14.9	82.2	0.88	13.0	80.0
0.13	16.0	83.4	0.07	14.4	83.3	0.12	12.6	81.1
0.10	15.8	83.6	0.10	14.6	86.1	0.08	12.4	82.3
0.10	15.9	86.9	0.09	14.7	89.2	0.07	12.1	82.1
0.11	16.0	90.0	0.15	14.8	90.6	0.10	12.4	83.9
0.18	16.0	94.4	0.22	14.5	92.8	0.24	10.6	89.8
0.20	15.8	93.8	0.06	13.9	84.3	0.26	10.6	92.9
0.14	15.5	88.1	0.18	14.8	93.9	0.10	10.2	87.5
0.18	15.0	93.2	0.31	14.1	94.3	0.28	10.4	88.3
0.26	14.8	93.9	0.24	12.3	93.8	0.22	8.6	93.7
0.26	13.8	93.7	0.28	11.0	93.8	0.17	6.8	93.9
0.28	12.5	95.3	0.15	11.4	79.5	0.16	5.4	92.6
0.97	12.1	80.9	0.14	12.3	88.7	0.09	9.9	88.2
0.11	9.1	89.4						

8.3 CIR-foam Project Site in Grundy County

To predict the moisture condition in the CIR-foam layer in Grundy County, a moisture loss index was developed as a function of the initial moisture content, the cumulative pavement temperature per hour as follows:

$$\triangle MC/hr = a_1 + a_2\ I_{MC} + a_3\ C_{Temp}/hr$$

Where,

I_{MC} = the actual moisture contents of CIR layer measured in the field using the embedded ECH_2O moisture sensor

C_{Temp} = cumulative pavement temperature (˚F) between moisture measurements

a_1, a_2, a_3 = multiple linear regression coefficients

Table 8-4 summarizes twenty-three sets at sensor A', thirty-one sets at sensor A, and twenty-eight sets at sensor B between rainfalls. As highlighted in Table 8-4, the data sets with the initial moisture content above 12% were removed from the further analysis because they are excessive moisture conditions which are beyond the moisture loss modeling range for CIR-foam projects. Consequently, seventeen sets of data points at sensor A', twenty-six sets of data points at sensor A, and eighteen sets of data points at sensor B were used for developing the moisture loss index.

As shown in the regression equation for each of three locations below, Δmoisture content per hour in CIR-foam layer can be predicted as a function of the initial moisture content and the cumulative pavement temperature per hour for the CIR-foam project site on County Road T-55, Grundy County, Iowa.

Sensor A': $\Delta MC/hr = -0.308 + 0.0363\ I_{MC} + 0.00256\ C_{Temp}/hr$ (R-square = 84.6%)
Sensor A: $\Delta MC/hr = 0.036 + 0.0410\ I_{MC} - 0.00156\ C_{Temp}/hr$ (R-square = 59.9%)
Sensor B: $\Delta MC/hr = -0.111 + 0.0370\ I_{MC} + 0.00041\ C_{Temp}/hr$ (R-square = 71.3%)

Overall, R-square values seemed to be reasonable and these equations are more reliable than the one developed earlier for the CIR-emulsion project.

Table 8-4. Summary of Δmoisture content/hour, initial moisture content, and cumulative pavement temperature/hour for CIR-foam project in Grundy County

			Sensor No					
A' (386+80)			A (386+80)			B (386-60)		
ΔMC /hour	Initial MC	C$_{Temp}$ /hour	ΔMC /hour	Initial MC	C$_{Temp}$ /hour	ΔMC /hour	Initial MC	C$_{Temp}$ /hour
0.19	5.9	96.8	0.25	6.5	95.5	0.06	4.2	89.6
0.09	4.6	79.0	0.10	5.1	82.8	0.06	3.7	86.3
0.11	4.6	90.5	0.10	5.0	89.9	0.04	3.0	95.6
0.06	3.3	100.8	0.08	4.2	98.4	0.10	4.0	78.9
0.59	21.5	89.0	0.09	5.4	80.7	0.04	3.7	91.6
0.81	21.4	87.6	0.06	5.5	92.1	0.39	12.7	87.3
0.30	9.0	88.8	0.08	6.0	88.5	0.27	9.4	87.2
0.08	5.0	82.7	0.10	5.3	88.2	0.07	5.1	82.8
0.10	4.7	87.9	0.06	4.6	83.2	0.09	5.0	87.0
0.09	4.1	97.7	0.10	5.1	89.1	0.07	4.1	95.2
0.72	17.1	83.4	0.11	5.1	94.7	0.40	16.3	77.3
0.15	7.8	86.1	0.54	16.9	87.5	0.91	19.0	84.9
0.14	7.0	86.4	0.10	5.9	88.4	0.18	6.6	86.6
0.08	5.2	77.9	0.22	5.2	86.1	0.09	5.5	85.4
0.11	5.6	89.2	0.13	4.8	89.8	0.05	4.0	79.2
0.50	12.5	85.9	0.21	4.7	80.2	0.08	4.8	87.8
0.13	12.5	72.8	0.10	4.9	73.7	0.35	15.6	79.4
0.50	12.8	81.6	0.16	5.3	104.2	0.56	14.6	85.9
0.22	8.4	89.9	0.08	4.7	83.6	0.29	9.3	90.6
0.10	5.7	88.0	0.13	4.4	79.3	0.17	6.7	87.7
0.10	5.1	89.9	0.31	12.1	88.3	0.16	6.3	88.9
0.08	4.6	91.4	1.54	13.0	75.0	0.13	5.7	90.0
0.05	3.6	87.9	0.17	8.7	87.6	0.24	4.5	88.1
			0.11	6.9	90.0	0.05	13.6	79.4
			0.11	5.6	103.8			
			0.14	5.5	82.0			
			0.16	5.4	77.6			
			0.06	5.1	91.0			
			0.05	4.9	93.2			
			0.04	4.5	88.7			
			0.46	11.6	74.9			

57

9. SUMMARY AND CONCLUSIONS

The previous research performed laboratory experiments to measure the impacts of the curing on the indirect tensile strength of both CIR-foam and CIR-emulsion mixtures. However, a fundamental question was raised during the previous research regarding a relationship between field moisture content and the laboratory moisture content. Therefore, during this research, both temperature and moisture conditions were measured in the field by embedding the sensors at a midpoint and a bottom of the CIR layer. The main objectives of the research are to: (1) measure the moisture levels throughout a CIR layer and (2) develop a moisture loss index to determine the optimum curing time of CIR layer before HMA overlay.

To develop a set of moisture loss indices, the moisture contents and temperatures of CIR-foam and CIR-emulsion layers were monitored for five months. The developed sets of moisture loss indices based on the field measurements will help pavement engineers determine an optimum timing of an overlay without continually measuring moisture conditions in the field using a nuclear gauge.

Conclusions

Based on the limited field experiment, the following conclusions are derived:

1. The moisture conditions of the CIR layer can be monitored accurately using a capacitance moisture sensor.

2. A set of moisture loss indices for CIR layers is a viable tool in determining the optimum timing for an overlay without measuring actual moisture contents.

3. Modulus measured by FWD seemed to be in a good agreement with the stiffness measured by geo-gauge.

4. The stiffness of CIR-foam layer increased as curing time increased. The layer stiffness seemed to be affected by the pavement temperature more than the moisture content.

5. The geo-gauge should be considered for measuring the stiffness of CIR-foam layer that can be used to determine the timing of an overlay.

Recommendations/Future Studies

1. To validate the moisture loss indices, six CIR construction sites that include two CIR-foam project sites, two CIR-emulsion (CSS-1) project sites and two CIR-emulsion (HFMS-2P) project sites, should be monitored using embedded moisture and temperature sensors.

2. To explore the concept of using CIR stiffness as a curing tool for determining an optimum timing for an overlay, the geo-gauge should be used to measure the stiffness of the above six CIR projects.

3. The moisture content measured in the field will be compared against the stiffness measured by the geo-gauge for a given temperature

REFERENCES

Hanek, G. L., M. A. Truebe, M. A. Kestler. *Evaluation Moisture Sensors and Monitoring Seasonal Moisture Variation in Low-Volume Roads*. Transportation Research Board of the National Academies, Washington D.C., 2001.

Jiang, Y. J., S. D. Tayabji. *Evaluation of In-Situ Moisture Content at Long-Term Pavement Performance Seasonal Monitoring Program Sites.* CD-ROM. Transportation Research Board of the National Academies, Washington D.C., 1999.

Liang, R. Y., K. Al-Akhras, *Field Monitoring of Moisture Variations under Flexible Pavement*. Transportation Research Board of the National Academies, Washington D.C., 2006.

Lee, S. I., D. G. Zollinger, R. L. Lytton, *Determination of Moisture Content of Soil Layers Using TDR Based on Micromechanics Approach*. Transportation Research Board of the National Academies, Washington D.C., 2008.

Yu, X., N. Liu, J. Gonzalez, X. B. Yu. *New Instrument and Analysis Method for Accurate Freeze-Thaw Measurement*. Transportation Research Board of the National Academies, Washington D.C., 2008.